© 2019. Published by The Company of Biologists Ltd | Development (2019) 146, dev180976. doi:10.1242/dev.180976

RESEARCH ARTICLE

Scribble and Discs-large direct initial assembly and positioning of adherens junctions during the establishment of apical-basal polarity

Teresa T. Bonello[1,*], Wangsun Choi[2] and Mark Peifer[1,3,4,*]

ABSTRACT

Apical-basal polarity is a fundamental property of animal tissues. *Drosophila* embryos provide an outstanding model for defining mechanisms that initiate and maintain polarity. Polarity is initiated during cellularization, when cell-cell adherens junctions are positioned at the future boundary of apical and basolateral domains. Polarity maintenance then involves complementary and antagonistic interplay between apical and basal polarity complexes. The Scribble/Dlg module is well-known for promoting basolateral identity during polarity maintenance. Here, we report a surprising role for Scribble/Dlg in polarity initiation, placing it near the top of the network-positioning adherens junctions. Scribble and Dlg are enriched in nascent adherens junctions, are essential for adherens junction positioning and supermolecular assembly, and also play a role in basal junction assembly. We test the hypotheses for the underlying mechanisms, exploring potential effects on protein trafficking, cytoskeletal polarity or Par-1 localization/function. Our data suggest that the Scribble/Dlg module plays multiple roles in polarity initiation. Different domains of Scribble contribute to these distinct roles. Together, these data reveal novel roles for Scribble/Dlg as master scaffolds regulating assembly of distinct junctional complexes at different times and places.

KEY WORDS: *Drosophila*, Scribble, Adherens junction, Apical-basal polarity

INTRODUCTION

Cell polarity is a fundamental property of cells, from yeast to neurons. Epithelial apical-basal polarity provides an example (Campanale et al., 2017). Precisely positioning polarity and junctional proteins at the plasma membrane allows cells to create domains with distinct biochemical properties, allowing, for example, intestinal cells to position glucose importers apically and glucose exporters basally. Cell-cell adherens junctions (AJs) reside at the boundary between apical and basolateral domains, and are key polarity landmarks. Once established, mutually exclusive apical and basal domains are maintained and elaborated by recruitment or antagonism between apical and basolateral polarity complexes, with remarkable conservation of function across species, although sometimes acting in different combinations.

Drosophila embryos provide a superb model for defining the mechanistic basis of apical-basal polarity establishment and maintenance (Harris, 2012). Development begins with 13 rounds of nuclear division without cytokinesis. The last four occur at the egg cortex, which provides a key polarity landmark to polarize the mitotic divisions. The plasma membrane then moves down around each nucleus, creating ~6000 cells. During cellularization, cell polarity is initially established, with cadherin-catenin complexes assembled into spot AJs (SAJs) at the boundary of what will become apical and basolateral domains. AJ proteins are not essential for syncytial divisions (Grevengoed et al., 2003), but in their absence cell adhesion and polarity are lost when gastrulation begins (Cox et al., 1996; Müller and Wieschaus, 1996; Sarpal et al., 2012; Tepass et al., 1996).

Focus then turned to defining mechanisms required to properly position and assemble AJs. The polarity regulator Bazooka (Baz; i.e. fly Par3) colocalizes with cadherin-catenin complexes and is required for their apical positioning and supermolecular assembly (Harris and Peifer, 2004; Müller and Wieschaus, 1996). An apical actin-based scaffold thought to anchor Baz and AJs apically and dynein-driven apical transport also play roles (Harris and Peifer, 2005). The actin-junction crosslinker Canoe (Cno; Afadin in fly) and its regulator, the GTPase Rap1, act upstream of both Baz and AJ positioning (Bonello et al., 2018; Choi et al., 2013). Apical activated Rap1 positions Cno at nascent SAJs where Cno directs Baz and AJ positioning.

Polarity is then maintained and increasingly elaborated via recruitment or antagonism between a complex network of apical and basolateral polarity complexes (Tepass, 2012). The apical domain is initially defined by the Par complex (aPKC/Par-6), which is recruited apically in a Baz- and cdc42-dependent fashion (e.g. Bilder et al., 2003; Harris and Peifer, 2005, 2007; Hutterer et al., 2004), and then acts in opposition to Par-1 to focus and position belt AJs (McKinley and Harris, 2012; Wang et al., 2012). The Crumbs complex is then localized and promotes apical membrane identity (reviewed by Bazellieres et al., 2018). The Par and Crumbs complexes antagonize apical localization of basolateral polarity proteins, while the basolateral Scribble (Scrib)/Discs-Large (Dlg)/Lethal giant larvae (Lgl) module and Yurt group act in parallel to prevent basolateral spread of apical and junctional proteins (Bilder et al., 2003; Laprise et al., 2006, 2009; Tanentzapf and Tepass, 2003). Much of this is mediated by phosphorylation – aPKC phosphorylation excludes basal proteins from the apical domain (reviewed by Hong, 2018) while Par-1 phosphorylation excludes apical proteins from the basolateral domain.

Here, we focus on the Scrib module (Stephens et al., 2018). Dlg and Lgl regulate tissue growth in imaginal discs, which are precursors of the adult epidermis (Gateff and Schneiderman, 1974; Woods et al.,

[1]Department of Biology, University of North Carolina at Chapel Hill, CB#3280, Chapel Hill, NC 27599-3280, USA. [2]Department of Pathology, Brigham and Women's Hospital and Harvard Medical School, Boston, MA 02115, USA. [3]Curriculum in Genetics and Molecular Biology, University of North Carolina at Chapel Hill, Chapel Hill, NC 27599, USA. [4]Lineberger Comprehensive Cancer Center, University of North Carolina at Chapel Hill, Chapel Hill, NC 27599, USA.

*Authors for correspondence (peifer@unc.edu; tbonello@live.unc.edu)

T.T.B., 0000-0002-3974-5611; M.P., 0000-0003-1412-3987

Received 29 May 2019; Accepted 14 October 2019

Development (2019) 146, dev180976. doi:10.1242/dev.180976

1996). Scrib promotes embryonic epithelial integrity (Bilder and Perrimon, 2000) and works with Dlg and Lgl in both epithelial polarity and growth regulation (Bilder et al., 2000). They are mutually required for one another's localizations, but whether they form a protein complex or act in parallel remains unclear. In the mature ectoderm, the Scrib-module antagonizes apical domain expansion and maintains AJs, with loss resulting in ectopic expansion of apical and AJ proteins along the basolateral axis (Bilder et al., 2000, 2003; Bilder and Perrimon, 2000; Tanentzapf and Tepass, 2003). Interestingly, later the Scrib module colocalizes with and is required for the assembly of core septate junction (SJ) proteins into functional SJs (Woods et al., 1996; Zeitler et al., 2004), which, like mammalian tight junctions, provide epithelial barrier function. Assembly of core SJ proteins is accompanied by enhanced immobilization on the cortex, a property not disrupted by Dlg loss (Oshima and Fehon, 2011). Thus, the Scrib module is required for SJ positioning and supermolecular assembly but not for SJ core complex formation. Dlg and its binding partner Strabismus also have a reported role in cellularization (Lee et al., 2003). Scrib and Dlg also regulate assembly/localization of other supermolecular complexes like neural synapses. Parallel work in *C. elegans* has revealed essential roles for the Scrib and Dlg orthologs for junctional function and polarity maintenance (Bossinger et al., 2001; Caria et al., 2018; Firestein and Rongo, 2001; Köppen et al., 2001; Legouis et al., 2000; Lockwood et al., 2008; Mathew et al., 2002; McMahon et al., 2001).

Work in cultured mammalian cells revealed parallel but distinct roles for Scrib in cell adhesion and polarity, regulating AJ formation/dynamics. Scrib localizes to the basolateral membrane, thus overlapping AJs though its localization relative to tight junctions remains less clear (e.g. Métais et al., 2005; Navarro et al., 2005). In MDCK cells, Scrib knockdown reduces Ecad-based adhesion and Ecad retention at AJs, and delays polarization, potentially via effects on p120-Ecad interactions and the Rho-GEF SGEF (Awadia et al., 2019; Lohia et al., 2012; Qin et al., 2005). Scrib also regulates polarization of MCF7 cells in 3D cysts (Hendrick et al., 2016). However, whereas mouse Scrib mutants have defects in neural tube and other tissues (Murdoch et al., 2003; Pearson et al., 2011; Yates et al., 2013; Zarbalis et al., 2004), often via effects on planar cell polarity (reviewed by Bonello and Peifer, 2019), they do not phenocopy loss of Ecad. Work from the Troyanovsky lab published while this paper was under review may provide an explanation. DLD1 cells knocked down for all three LAP family proteins – Scrib, Erbin and Lano – exhibit much more severe defects in assembly of apical junctions (Choi et al., 2019) and apical-basal polarity.

Our goal is to define the mechanisms that direct polarity establishment, with the ultimate objective being to define the full protein network involved. While the data above are sometimes portrayed as a simple linear pathway – Rap1GEFs→Rap1→Cno→Baz→AJs→proteins involved in polarity elaboration – things are more complex. For example, Cno is 'upstream' of Baz and aPKC, but their loss perturbs Cno supermolecular assembly (Choi et al., 2013). Wiring of the polarity system also varies significantly between different tissues. Here, we explore the roles of Scrib and Dlg. In contrast to the idea that they are primarily involved in polarity elaboration and maintenance, we find they play a crucial role in polarity establishment, acting at the top of the known hierarchy.

RESULTS

Scrib and Dlg are enriched near nascent AJs during cellularization

Polarity establishment begins at cellularization (stage 5), at the end of which Baz and AJs are positioned apically. At gastrulation onset (stage 6), additional polarity regulators come into play, successively elaborating polarity. In the canonical model, apical Crumbs, Yurt and Par6/aPKC complexes, and the basolateral Scrib module and Par-1 reinforce and elaborate polarity by mutual antagonism. In the mature ectoderm, Scrib and Dlg localize basolateral to AJs (Fig. 1A, quantified in B), where they are known to overlap with SJs. Core SJ proteins such as Coracle and Neurexin do not localize until mid-embryogenesis (Baumgartner et al., 1996; Fehon et al., 1994). If the roles of Scrib/Dlg were restricted to polarity elaboration and maintenance, one might expect they would not localize until gastrulation onset, when polarity elaboration begins, and that they then would be basolateral to AJs. However, Dlg localizes to the lateral membrane prior to SJ formation, and in fact is found all along the lateral domain as early as cellularization when polarity is established, overlapping the forming AJs (Woods and Bryant, 1991; Lee et al. 2003; Harris and Peifer, 2004; Sokac and Wieschaus, 2008). We therefore compared localization of Scrib to that of Dlg at this stage.

As cellularization proceeds, cadherin and the catenins localize to an apicolateral position in punctate SAJs (Fig. 1C, cyan arrows). AJ proteins also localize to smaller puncta along the lateral membrane, and are enriched in basal junctions (BJs; Fig. 1C, magenta arrows). Cno localization is largely restricted to nascent SAJs (Fig. 1E). In contrast to later Scrib and Dlg basolateral SJ localization, in cellularizing embryos both extended the entire length of the lateral membrane (Fig. 1C″,E″), although neither was enriched with F-actin/myosin at the furrow front. More surprising, Dlg and Scrib extended apically to overlap nascent SAJs, and by late cellularization there was enrichment of both Dlg (Fig. 1C″, cyan arrow) and Scrib (Fig. 1E″, cyan arrow) in a restricted region overlapping the nascent SAJs. Maximum intensity projections (MIPs) of multiple cross-sectional planes further emphasized this (Fig. 1C‴,E‴). The degree of enrichment was revealed by traces of intensity along the apical basal axis (Fig. 1H) or by quantification of pixel intensity in the region of the nascent SAJs versus the basolateral region (Fig. 1I; see Fig. S1A,B for details). *En face* views revealed that, while AJ proteins and Cno localize discontinuously to SAJs (Fig. 1F′; Fig. S2A′), Scrib and Dlg localize relatively uniformly around the circumference of the cell (Fig. 1F″; Fig. S2A″,B″). While Cno and other AJ proteins are enriched at tricellular junctions (Bonello et al., 2018), Dlg (Fig. S2C,D) and Scrib (Fig. 1G,N) are not. Apical Dlg and Scrib enrichment became even more pronounced as gastrulation began (stage 6; Fig. 1D-D″,L-L″, cyan arrows). Once again, MIPs (Fig. 1M) and pixel quantification (Fig. 1J) emphasized this. By stage 7, AJ proteins and Cno move apically and tighten in their localization, thus initiating separation from the site where Scrib is enriched (Fig. 1K). These data prompted us to consider the possibility that Scrib/Dlg might already have roles during polarity establishment rather than exclusively during polarity maintenance.

Baz and Rap1 play roles in Dlg apical enrichment while AJ assembly is not essential

The close spatial relationship of SAJs, Dlg and Scrib during cellularization prompted us to investigate their functional interdependency. We first considered the hypothesis that proteins that position AJs are necessary for apical enrichment of Dlg and Scrib. Baz and Rap1/Cno regulate AJ positioning (Choi et al., 2013; Harris and Peifer, 2004). We thus examined whether they regulate apical Dlg enrichment. We assessed two enrichment parameters, quantifying cortical enrichment in the SAJ region versus the basolateral region (Fig. S1B), and also examining effects on the tight enrichment of Dlg at the level of the SAJs. In wild type, tight

Development (2019) 146, dev180976. doi:10.1242/dev.180976

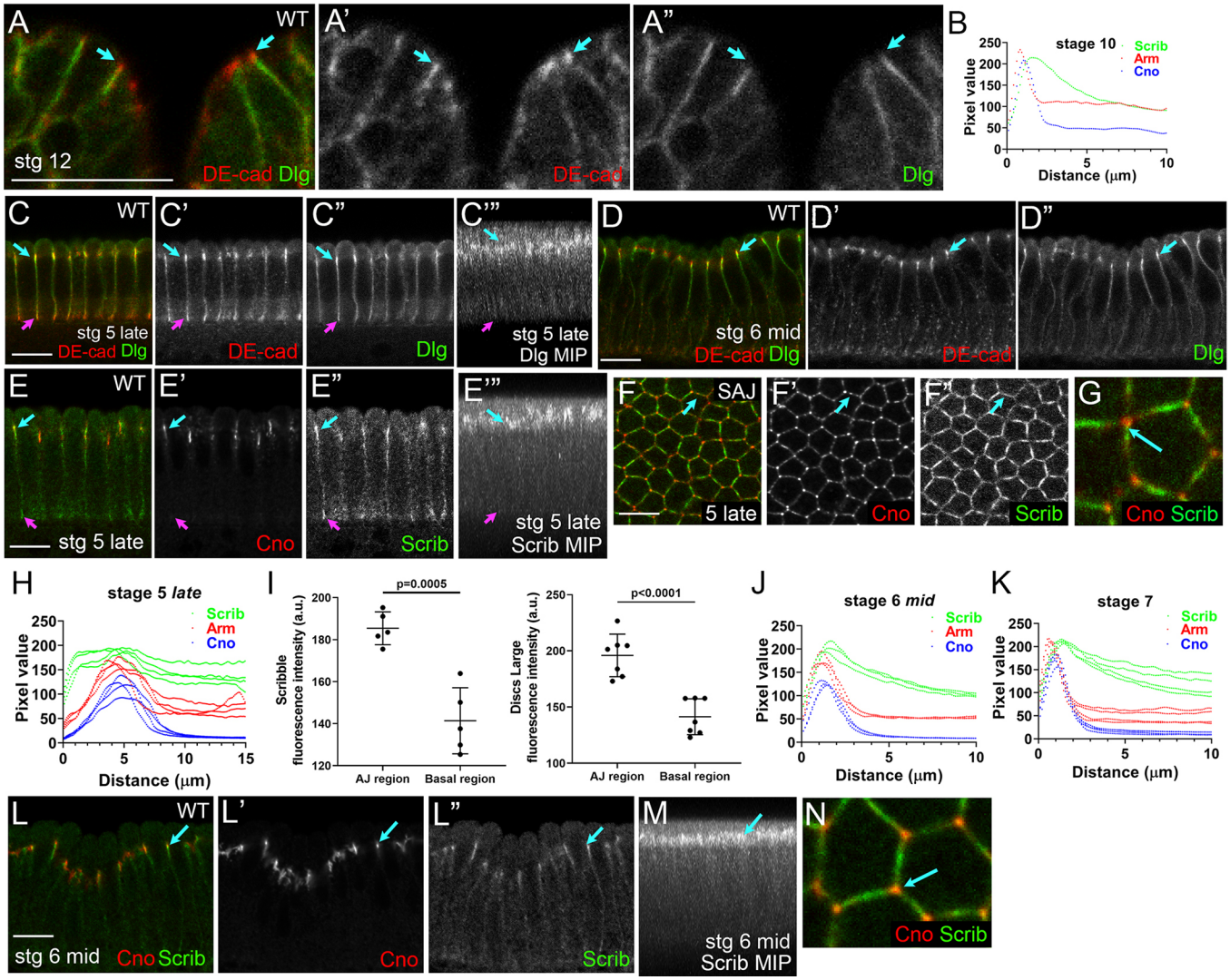

Fig. 1. Scrib and Dlg localize to nascent AJs during cellularization. (A-A″) Stage 12 ectoderm. Dlg localizes to septate junctions, basal to AJs. (B) Quantification at stage 10. Pixel plots along the apical-basal axis reveal separation. (C-J,L-N) Cellularization to early gastrulation. Dlg (C-D″) and Scrib (E-G,L) localization relative to SAJs. (C-E″,L) Cross-sections. (F-G,N) *En face* sections through SAJs at the level of highest enrichment. (C‴,E‴) Maximum intensity projections (MIPs). (C-C″,E-E″) Dlg and Scrib localize along the basolateral membrane during cellularization, overlapping both SAJs (cyan arrows) and BJs (magenta arrows). (F) At the SAJ level, Scrib is uniformly distributed around the cell circumference without TCJ enrichment (G,N, cyan arrows). (D-D″,L-L″,M) Gastrulation. Dlg and Scrib remain enriched near apical SAJs (cyan arrows). (H,J,K) Quantification via pixel plots reveals the changing localization of Scrib relative to AJ proteins. (I) Quantification of relative levels of cortical Scrib and Dlg at the SAJ level versus basolateral. Data are mean±s.d. with individual data points indicated. Scale bars: 10 µm.

apical enrichment at the level of SAJs was consistently observed (Fig. 2A,D, arrows; seen in 21/22 embryo cross-sections) and Dlg mean fluorescence intensity was 1.60 times higher in the apical cortex (Fig. 2G). A previously validated *Rap1* RNAi construct (Bonello et al., 2018) significantly reduced but did not eliminate Dlg apical enrichment: tight apical enrichment was seen in only 5/8 embryo cross-sections (Fig. 2B, arrow, versus C) and Dlg fluorescence intensity was only 1.44 times higher in the apical cortex (Fig. 2G). *baz* RNAi (validated in Fig. S2E) resulted in an even more pronounced change in Dlg apical enrichment: tight apical enrichment was lost (Fig. 2E; 0/9 embryo cross-sections observed), even at stage 6 (Fig. 2F), while Dlg fluorescence intensity was only 1.47 times higher in the apical cortex (Fig. 2G). Thus, both Rap1 and Baz help regulate Dlg apical enrichment, with Baz being particularly important for the strong elevation at the level of nascent SAJs.

We next examined whether AJ proteins are required for Dlg apical enrichment. To do so, we knocked down maternal and zygotic Arm (*Drosophila* β-catenin) using RNAi (Fig. S2F). β-Catenin is required to traffic E-cad to the plasma membrane in mammals and *Drosophila* (Chen et al., 1999; Harris and Peifer, 2004). *arm-RNAi* or mutation substantially reduces plasma membrane DE-cad (Harris and Peifer, 2004); DE-cad is lost from SAJs and BJs, and localizes to puncta aligned along the basolateral membrane and in an apical compartment above the nucleus (Fig. 2A versus H), consistent with a trafficking defect. This continues during early gastrulation (Fig. 2J). However, tight apical Dlg enrichment at the level of SAJs was not perturbed (Fig. 2H″,J″, observed in 12/13 embryos), and enrichment of Dlg in the apical cortex was unchanged (Fig. 2N). This is consistent with previous work showing that Scrib is not lost from the plasma membrane in *arm* maternal/zygotic mutants later in development (Bilder et al., 2003).

Development (2019) 146, dev180976. doi:10.1242/dev.180976

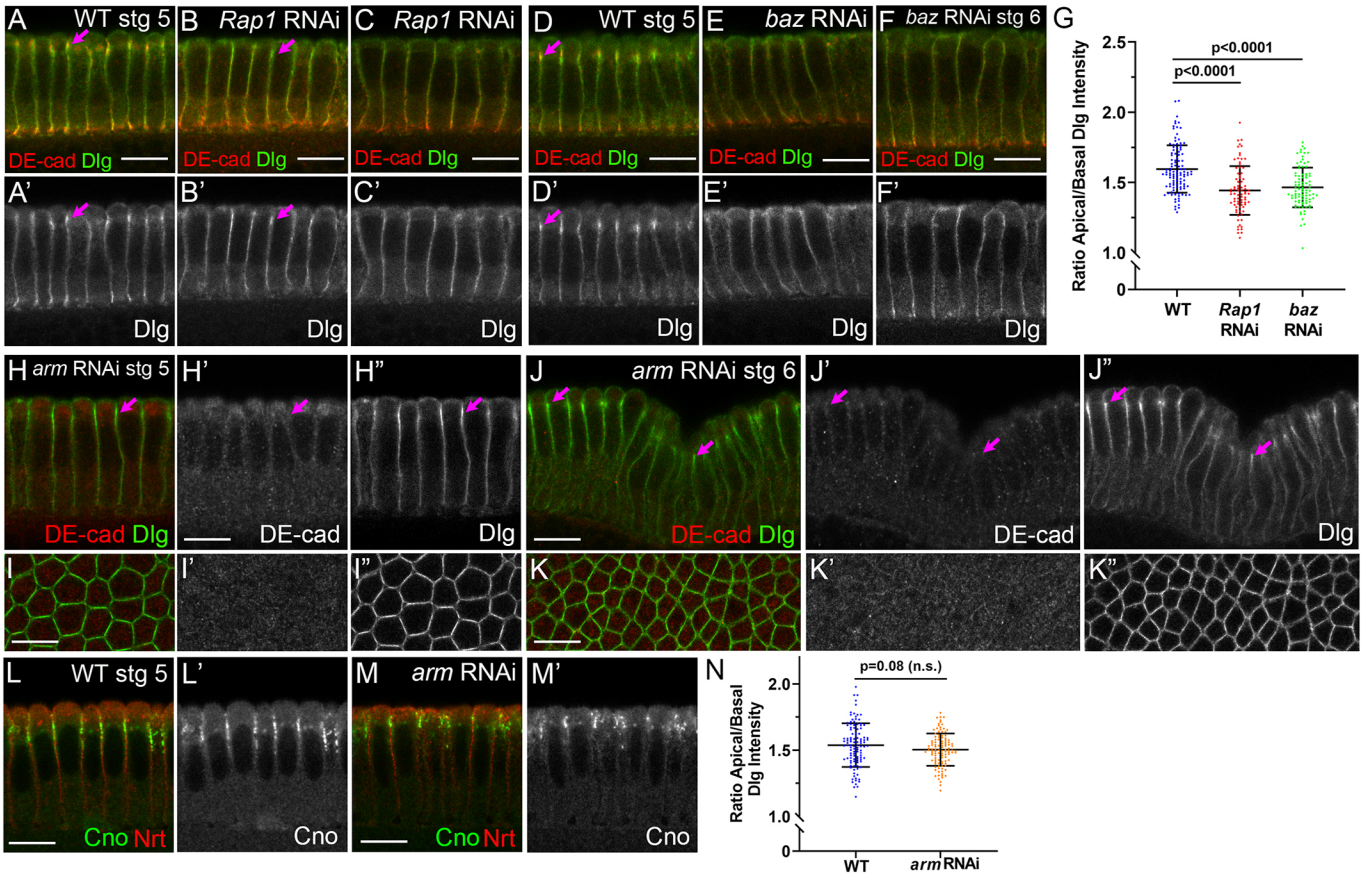

Fig. 2. Assessing roles for Rap1, Baz and AJs in Dlg enrichment at the level of nascent SAJs. Dlg or Cno localization at end of cellularization (A-E′,H-I″,L-M′) or at gastrulation onset (F,F′,J-K″) in wild type or embryos expressing *Rap1*, *baz* or *arm-RNAi*. (H-K″) Embryos co-stained with DE-cad to verify junctional disruption after *arm-RNAi*. Arrows indicate apical SAJs. (A,A′,D,D′) Wild type. There is tight apical enrichment of Dlg at nascent SAJs (arrows). This is less consistently observed after *Rap1-RNAi* (B-C′) and is lost after *baz-RNAi* (E-F′). (G) *Rap1-RNAi* and *baz-RNAi* reduce apical cortical enrichment of Dlg (mean±s.d.). (H-K″) Tight apical enrichment of Dlg at nascent SAJs is retained after *arm-RNAi* (H-J″, arrows; I-K″, *en face* sections at SAJs). (L-M′) *arm-RNAi* does not eliminate apical restriction of Cno. (N) *arm-RNAi* does not reduce apical cortical enrichment of Dlg. Data are mean±s.d. with individual data points indicated. Scale bars: 10 µm.

Interestingly, Cno and Baz positioning also do not require AJ function (Fig. 2L versus M; Harris and Peifer, 2004; Sawyer et al., 2009). These data suggest AJ assembly is not essential for Dlg apical enrichment at polarity establishment, consistent with the possibility that Scrib/Dlg act upstream.

Scrib and Dlg are essential for positioning AJs during polarity establishment

Polarity establishment begins with SAJ positioning and supermolecular assembly. Small cadherin-catenin clusters originating from the apical surface must be correctly positioned at the interface between apical and basolateral domains. Next, they organize into larger supermolecular assemblies (McGill et al., 2009). These are distributed around the circumference, with some enrichment at TCJs. AJ positioning requires Baz, an intact actin cytoskeleton, dynein-directed microtubule transport, and the small GTPase Rap1 and its effector Cno.

The surprising enrichment of Scrib/Dlg near nascent SAJs led us to examine whether they play roles during early polarization. To test this, we maternally expressed small hairpin RNAs against *scrib* and *dlg* to reduce both maternal and zygotic transcripts. We found effective shRNAs for each, which reduced protein levels below the detection threshold of immunoblotting (Fig. S2G-J; interestingly, knockdown of one did not alter levels of the other), and replicated known cuticle phenotypes (Fig. S3A-D). These included two *scrib* shRNAs targeting different regions of the mRNA, reducing likelihood of off-target effects.

In wild type, cadherin-catenin assembly into apical SAJs begins early in cellularization (Fig. 3A, red arrow), and by mid-late cellularization AJs proteins are strongly enriched there (Fig. 3A′,A″, red arrows; quantified in G,H). Our standard heat-fixation procedure emphasizes stably associated junctional proteins over the diffuse cytoplasmic pool, making this clearer. This enrichment becomes even clearer in MIPs of multiple cross-sectional planes (Fig. 3A‴, red arrows). Cadherin-catenin complexes also accumulate in smaller puncta along the lateral membrane (Fig. 3A-A‴, cyan arrows), and are enriched just apical to the furrow front in BJs (Fig. 3A-A‴, yellow arrows; Hunter and Wieschaus, 2000). Both *scrib-RNAi* (Fig. 3B-B‴) and *dlg-RNAi* (Fig. 3C-C‴) caused pronounced AJ protein mislocalization; Arm localized to small puncta distributed nearly evenly along the apical-basal axis. To quantify this, we measured pixel intensities along the apical-basal axis from MIPs and displayed these as heat maps (Fig. 3G). We also calculated the ratio of pixel intensity of Arm in the SAJs versus in the basolateral region (see Fig. S1A for details). This revealed that although Arm is roughly twofold enriched in the SAJ relative to the basolateral cortex in wild type, this enrichment is essentially lost after *scrib-RNAi* (Fig. 3H). Interestingly, AJ puncta not only spread basally

Development (2019) 146, dev180976. doi:10.1242/dev.180976

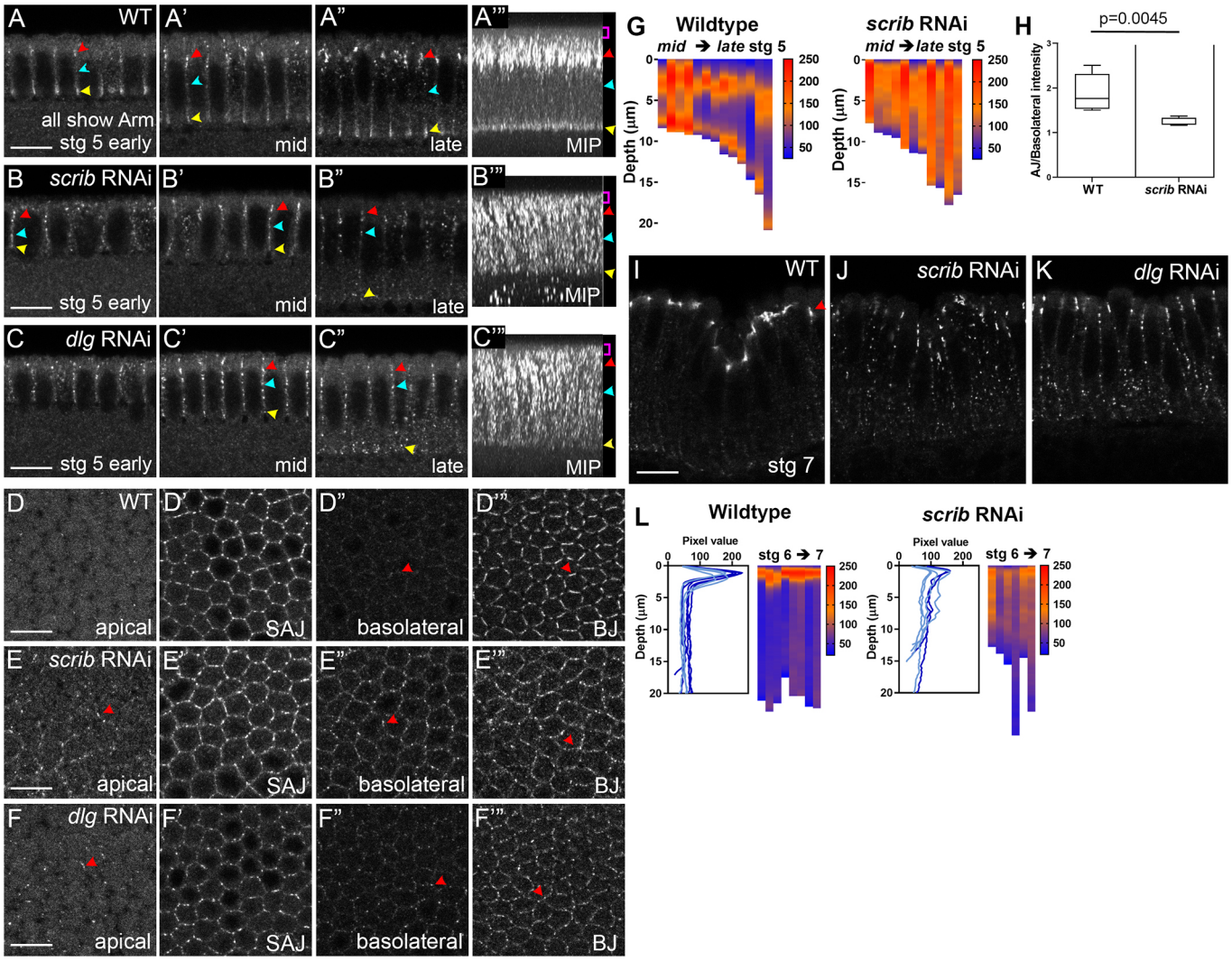

Fig. 3. Scrib and Dlg are required for SAJ apical positioning and organization. (A-C″,I-K) Cross-sections. (A‴,B‴,C‴) MIPs. (D-F″) *En face* sections through apical membrane (0 µm), SAJs (−3.6 µm), basolateral membrane and basal junctions (BJs), where red arrowheads indicate altered Arm localization or organization compared with wild type. (G,L) Heat maps. Arm puncta displacement along apical-basal axis, from MIPs, with pixel intensity plotted against distance from apical surface. Vertical bars indicate individual embryos. *scrib-RNAi* (B,E,J) or *dlg-RNAi* (C,F,K) disrupt Arm polarization during cellularization and gastrulation. Arm does not effectively enrich at apical SAJs (B-C‴, red arrowheads) or BJs (yellow arrowheads) and accumulates in puncta along the basolateral membrane (cyan arrowheads). (G) Heat maps showing Arm distribution from mid- to late-cellularization. (H) *scrib-RNAi* significantly reduces Arm enrichment in SAJs versus basolateral domain. Box and whisker plot (median, upper and lower quartile limits, and range). (I-K) Arm mislocalization after *scrib-RNAi* and *dlg-RNAi* persists during gastrulation (stage 7). (L) Arm distribution at stage 6-7. Scale bars: 10 µm.

(Fig. 3B-B‴, C-C‴, cyan arrows, D″ versus E″,F″) but also mislocalize into the apical domain (Fig. 3A‴ versus B‴ and C‴, brackets, D versus E,F).

A second junctional pool forms near the furrow tip (Fig. 3A-A‴, yellow arrows). BJs contain core AJ proteins, but unlike SAJs do not contain Cno or Baz. BJs are regulated by the cellularization-specific protein Nullo, and disassemble at gastrulation onset (Hunter and Wieschaus, 2000). We were surprised to find that after *scrib-RNAi* or *dlg-RNAi*, BJs also failed to form (Fig. 3A-A‴ versus B-B‴ and C-C‴, yellow arrows). Unlike punctate SAJs, in BJs Arm/DE-cad form linear arrays along bicellular contacts and are excluded from TCJs (Fig. 3D‴). After *scrib-RNAi* or *dlg-RNAi*, these arrays were disrupted (Fig. 3E‴,F‴).

As gastrulation initiates, cadherin-catenin complexes in SAJs move apically and focus (Fig. 3I arrow, quantified in L) as BJs disassemble. After *scrib-RNAi*, AJ mislocalization became even more pronounced at gastrulation onset – small cadherin-catenin complexes localized along the lateral membrane with little apical enrichment (Fig. 3J, quantified in L). Similar defects were seen after *dlg-RNAi* (Fig. 3K). Thus Scrib and Dlg play important roles in positioning and promoting supermolecular assembly of both SAJs and BJs.

Scrib/Dlg loss disrupts Cno localization but Cno continues to colocalize with AJ proteins

Apical restriction of both Baz and AJs requires Cno and its regulator Rap1. We thus examined whether Scrib/Dlg are required to apically position Cno. Cno colocalizes with Arm and Baz in SAJs from mid-late cellularization (Fig. 4A,B, brackets), and is especially enriched at TCJs (Fig. 4G′, arrows), where it forms cable-like structures (Bonello et al., 2018). Unlike core AJ proteins, Cno puncta are not found basolateral to SAJs or in BJs (Fig. 4B″, red arrow, quantified in I,J). *scrib-RNAi* disrupted this tight apical restriction during mid- (Fig. 4A versus C, brackets) and late cellularization (Fig. 4B versus

Development (2019) 146, dev180976. doi:10.1242/dev.180976

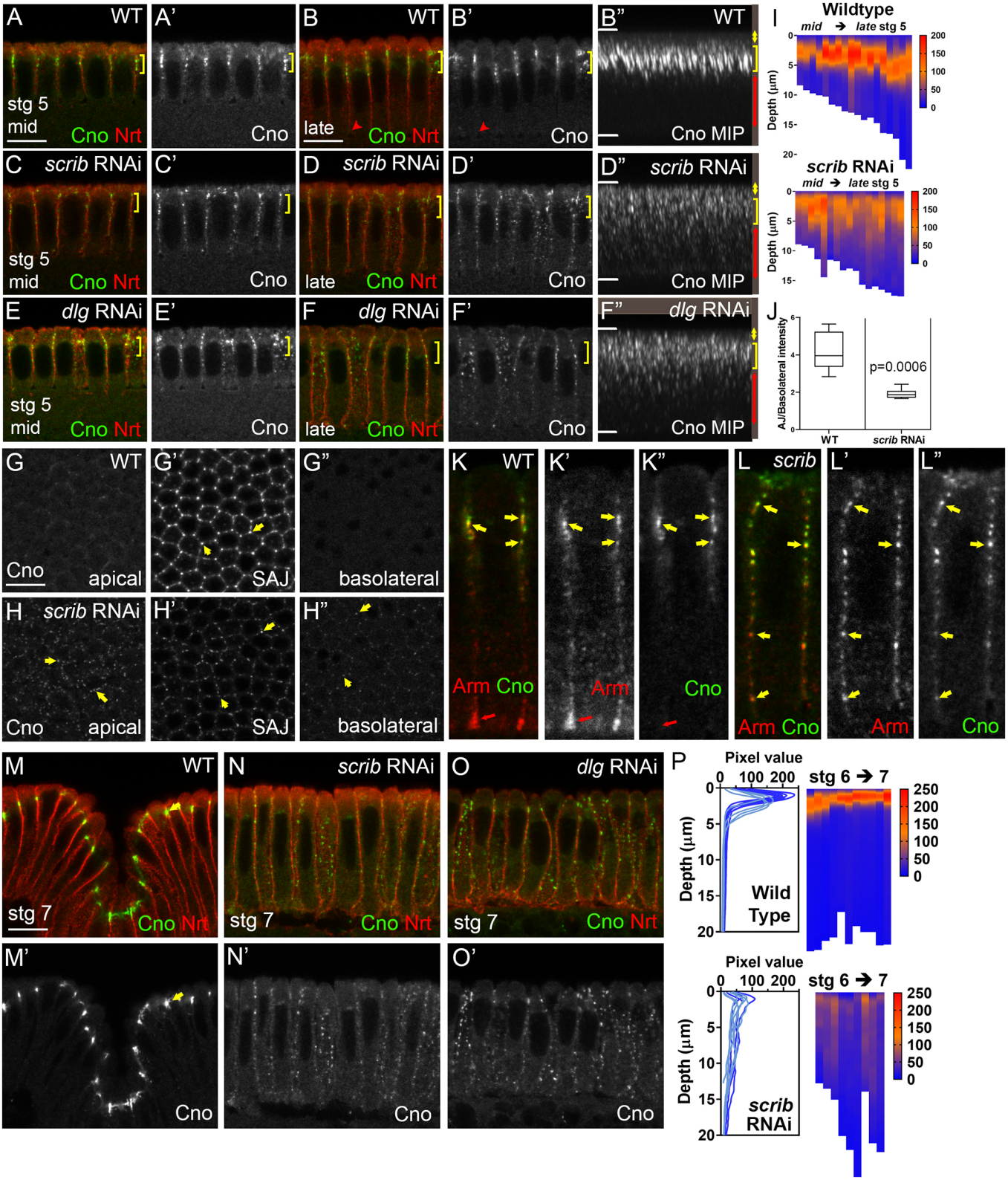

Fig. 4. Cno mislocalizes with Arm puncta. (A-F′,K-O′) Cross-sections. (B″,D″,F″) MIPs. (G-H″) *En face* sections through apical membrane (0 µm), SAJs (−3.6 µm) or basolateral membrane. (I,P) Heat maps from MIPs showing Cno puncta displacement along the apical-basal axis. Vertical bars indicate individual embryos. (A-L″) Cno enrichment at SAJs (A-B″,G-G″,K-K″,M,M′, yellow brackets and arrows) is disrupted after *scrib-RNAi* (C-D″,H-H″,L-L″,N,N′) and *dlg-RNAi* (E-F″,O,O′). (A-H″) Cno puncta mislocalize both apically and basolaterally during cellularization. Cno is not effectively organized at TCJs (G′,H′). (I,J) Corresponding quantification: heat maps (I) or degree of enrichment in SAJs relative to basolateral region (J, box and whisker plot; data are median, upper and lower quartile limits, and range). (K-L″) Mislocalized Cno puncta track with Arm (yellow arrows). (M-O′) Cno mislocalization is enhanced during gastrulation (stage 7), with displacement along the basolateral domain. (P) Quantification. Scale bars: 10 µm.

Development (2019) 146, dev180976. doi:10.1242/dev.180976

D, brackets). Cno puncta extended both apical (Fig. 4B″ versus D″, yellow arrows, G versus H) and basal to the usual position of SAJs (Fig. 4B″ versus D″, red arrows, G″ versus H″), though remnant apical enrichment in the top half of the cortex remained (quantified in Fig. 4I, J; Fig. S1A). Cno organization into apical supercellular cables was also lost (Fig. 4B″ versus D″, brackets), and strong TCJ enrichment was substantially reduced but not lost (Fig. 4G′ versus H′). *dlg-RNAi* had very similar effects (Fig. 4E,F).

We next asked whether misplaced AJ proteins remained associated or became randomly distributed with respect to one another. In wild-type, Cno and Arm colocalize in apical SAJs (Fig. 4K, yellow arrows), though Cno is more enriched at TCJs and is not included in BJs (Fig. 4K, red arrows). After *scrib-RNAi*, mislocalized Cno and Arm puncta showed clear colocalization in puncta along the entire length of the membrane (Fig. 4L, arrows), although the relative intensity of Arm is higher basally. This suggests that Scrib or Dlg loss does not affect basic molecular assembly of AJ complexes, but rather supermolecular assembly and retention at the apicolateral boundary.

In wild type, Cno and AJs move apically at gastrulation onset and tighten into belt AJs (Fig. 4M, arrow). Effects of *scrib-RNAi* on Cno became even more pronounced at gastrulation onset. Tight enrichment at apical AJs was completely lost, and instead Cno localized along the apical-basal axis (Fig. 4N, quantified in Fig. 4P). Some embryos retained residual apical enrichment (Fig. 4P) – these may be embryos receiving one rather than two copies of the shRNA construct. *dlg-RNAi* similarly disrupted Cno apical enrichment (Fig. 4O). Thus, Scrib/Dlg are essential for proper Cno assembly into apical AJs and its retention there during gastrulation.

Scrib loss reduces both Bazooka cortical localization and apical clustering

AJ positioning requires Baz function. In its absence, SAJs fail to assemble and cadherin-catenin complexes localize along the lateral membrane. Cno and localized Rap1 activity are required to effectively polarize Baz. Like Cno, Baz localizes in nascent SAJs, and, unlike cadherin-catenin complexes, does not localize further basally (Fig. 5A, brackets). We therefore asked whether Scrib was essential for directing Baz localization. *scrib-RNAi* led to substantial reduction in cortical Baz (Fig. 5A versus B, intensity matched from same experiment; quantified in C; Fig. S1C). In contrast, immunoblotting revealed that total Baz levels were at most modestly reduced (Fig. S2E). When we elevated the Baz signal to visualize the remaining Baz, we found its tight confinement to SAJs was also reduced after *scrib-RNAi* (Fig. 5D″ versus E″, quantified in D‴ versus E‴,G, Fig. S1C), with cortical Baz puncta now seen in the basolateral region (Fig. 5E″, blue arrows). However, Baz depolarization was more limited than that seen after Rap1 knockdown (Fig. 5F-G), in which Cno cortical localization is completely lost (Bonello et al., 2018). Thus, the modest pool of Cno retained apicolaterally after *scrib-RNAi* may be sufficient to partially support apical Baz enrichment, albeit at reduced levels and with impaired clustering. Disruption of Baz localization intensified as gastrulation began. Junctional maturation and regulation differ dorsally and ventrally in wild type (e.g. Wang et al., 2012), and effects of *scrib-RNAi* on Baz also differ, with puncta spread along the lateral membrane dorsally (Fig. 5H versus I) and lacking tight apical localization ventrally (Fig. 5J versus K). Even more striking, the remaining Baz puncta were not arrayed around the lateral membrane, as in wild type (Fig. 5L), but formed irregular clusters (Fig. 5M). These were often on dorsal/ventral cell boundaries (Fig. 5M, arrows), potentially reflecting the normal planar polarization of Baz (Fig. 5L, arrows). Thus, Scrib is essential for correctly assembling Baz into nascent SAJs and retaining it in intact junctions as gastrulation begins.

Loss of polarity and epithelial integrity rapidly intensify during gastrulation onset, and Arm and Cno colocalize in fragmented junctions

In the absence of Scrib, epithelial integrity is strongly disrupted (Bilder and Perrimon, 2000), but how rapidly this occurs remains unclear. We thus followed *scrib-RNAi* embryos through gastrulation. In some mutants, including *cno* and *Rap1* (Choi et al., 2013), other mechanisms are activated at gastrulation onset to largely restore apical restriction of AJs and Baz. There was no polarity rescue after Scrib/Dlg knockdown. In wild type, by stage 9 Arm, Cno and Baz colocalize in apical AJs (Fig. 6A,C,G, arrows), and only small Arm puncta are seen more basally (Fig. 6D). In contrast, *scrib-RNAi* cells began to separate apically (Fig. 6E, magenta arrow), AJs were fragmented but Arm and Cno largely colocalized in these fragments (Fig. 6E,F, cyan arrows). Baz was even more disrupted, with strong localization limited to larger junctional fragments (Fig. 6H,I, cyan versus magenta arrows). After *scrib-RNAi*, cortical actin was altered apically, with F-actin-rich protrusions near the apical surface (Fig. 6J,K), a phenotype also seen in embryos with reduced activity of the formin Diaphanous (Homem and Peifer, 2008) or expressing dominant-negative Rab11 (Roeth et al., 2009). The common phenotype after different perturbations suggests that correctly organized AJs restrain actin-driven protrusive behavior. When we followed *scrib-RNAi* embryos to much later stages (e.g. stage 13/14), we observed partial rescue of polarity, with return of Arm and Cno to apical junctions of epithelial balls and folded fragments (Fig. S3I), consistent with earlier work (Laprise et al., 2009).

Scrib/Dlg do not regulate cytoskeletal polarization during cellularization and blocking Rab5 using a dominant-negative mutant does not mimic loss of Scrib/Dlg

The cytoskeleton of cellularizing embryos is distinctly polarized (Mavrakis et al., 2009; Schmidt and Grosshans, 2018), reflecting establishment of cytoskeletal polarity during syncytial divisions. Actin is organized into distinct pools: actin-rich microvilli are seen apically, actin lines the basolateral cortex (Fig. S4A′) and actin (Fig. S4A, arrow, A″) and myosin (Fig. S4G,I,K,M, arrows) are strongly enriched at the furrow front. Some probes suggest a pool of actin is enriched at apical TCJs (e.g. Sawyer et al., 2009). Microtubules form inverted baskets over each nucleus (Fig. S4D-D″), with nucleation from apical centrosomes. Baz/AJ positioning during cellularization requires both an apical actin scaffold and dynein-mediated retrograde transport (Harris and Peifer, 2005). One mechanism by which Scrib/Dlg knockdown could affect Baz and AJ localization is by disrupting this polarized cytoskeletal organization. However, after *scrib-RNAi* or *dlg-RNAi*, F-actin (Fig. S4B,C), myosin (Fig. S4H,J,L,N) and α-tubulin (Fig. S4E,F) localization appeared unperturbed during cellularization, although, as noted above, actin organization is altered after gastrulation. Thus, Scrib/Dlg do not affect initial AJ positioning by disrupting overall cytoskeletal organization during cellularization.

Scrib regulates protein trafficking in imaginal discs and other contexts (reviewed by Bonello and Peifer, 2019), dynein-dependent trafficking maintains AJ/Baz positioning during cellularization (Harris and Peifer, 2005), and during later stages DE-cad can traffic through early endosomes (Roeth et al., 2009). We thus examined the hypothesis that Scrib acts to organize apical AJs by trafficking DE-cad. The early endosome marker Rab5 and the recycling

Development (2019) 146, dev180976. doi:10.1242/dev.180976

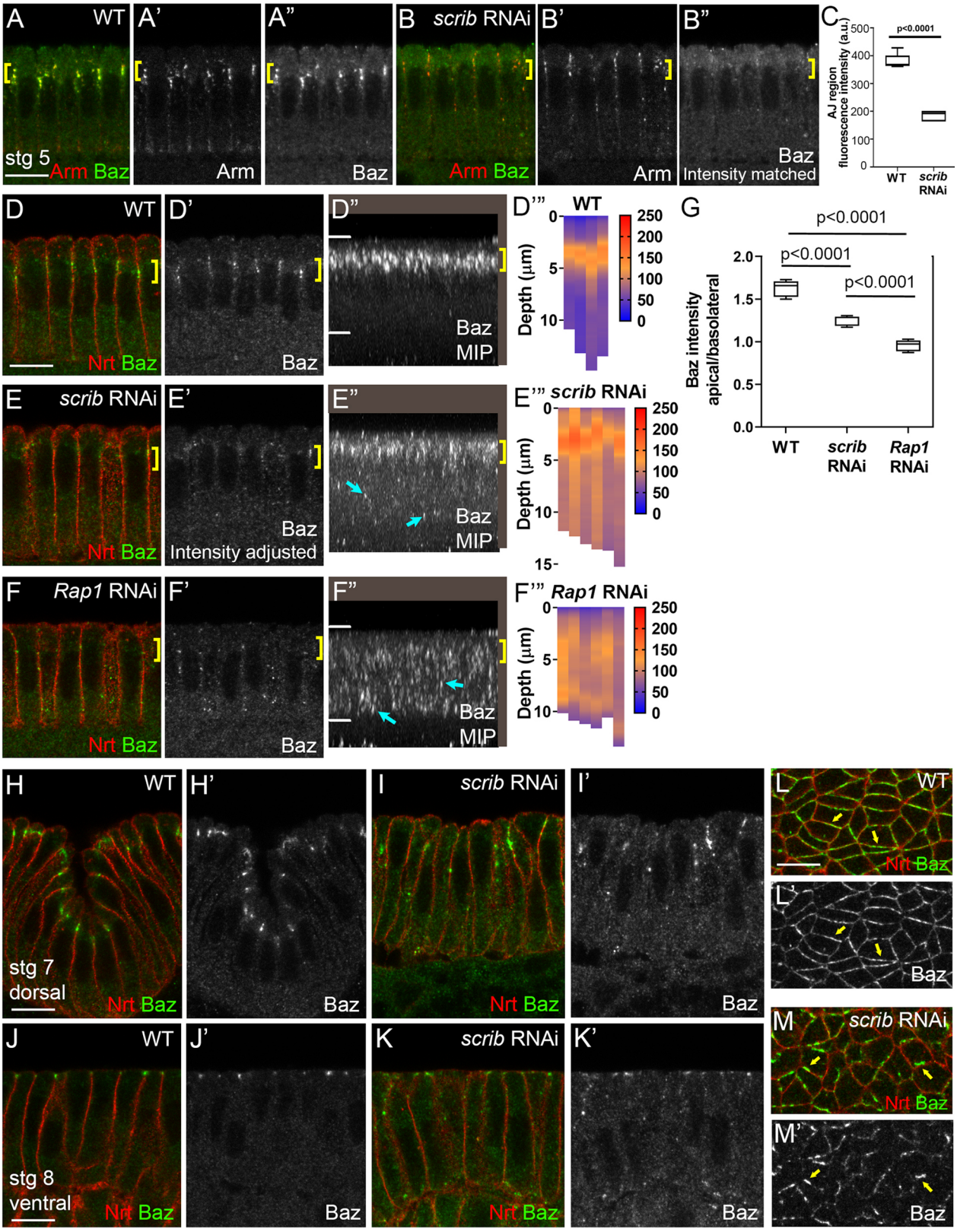

Fig. 5. Scrib is required for Baz cortical retention and apical clustering. (A-B″) Intensity matched images showing Arm and Baz in *scrib-RNAi* versus wild type. *scrib-RNAi* impairs Baz cortical retention during cellularization (yellow brackets). (C) Quantification of cortical Baz (data are median, upper and lower quartile limits, and range). (D,D′,E,E′,F,F′) Intensity-adjusted images, Baz during cellularization. (D″,E″,F″) MIPs. Apical Baz retention (yellow brackets) is reduced after *scrib-RNAi* (E), with ectopic puncta observed basolaterally (E″, cyan arrows) – this is distinct from the complete loss of Baz apical retention after *Rap1-RNAi* (F″). (D‴,E‴,F‴,G) Quantification of pixel intensities along the apical-basal axis. (G) Box and whisker plots; data are median, upper and lower quartile limits, and range. (H-K′) After gastrulation onset, Baz is lost from AJs and displaced as small puncta along the apical-basal axis in *scrib-RNAi*. (L-M′) *En face* sections through AJs at stage 7. Baz circumferential distribution becomes more irregular (yellow arrows). Scale bars: 10 µm.

Development (2019) 146, dev180976. doi:10.1242/dev.180976

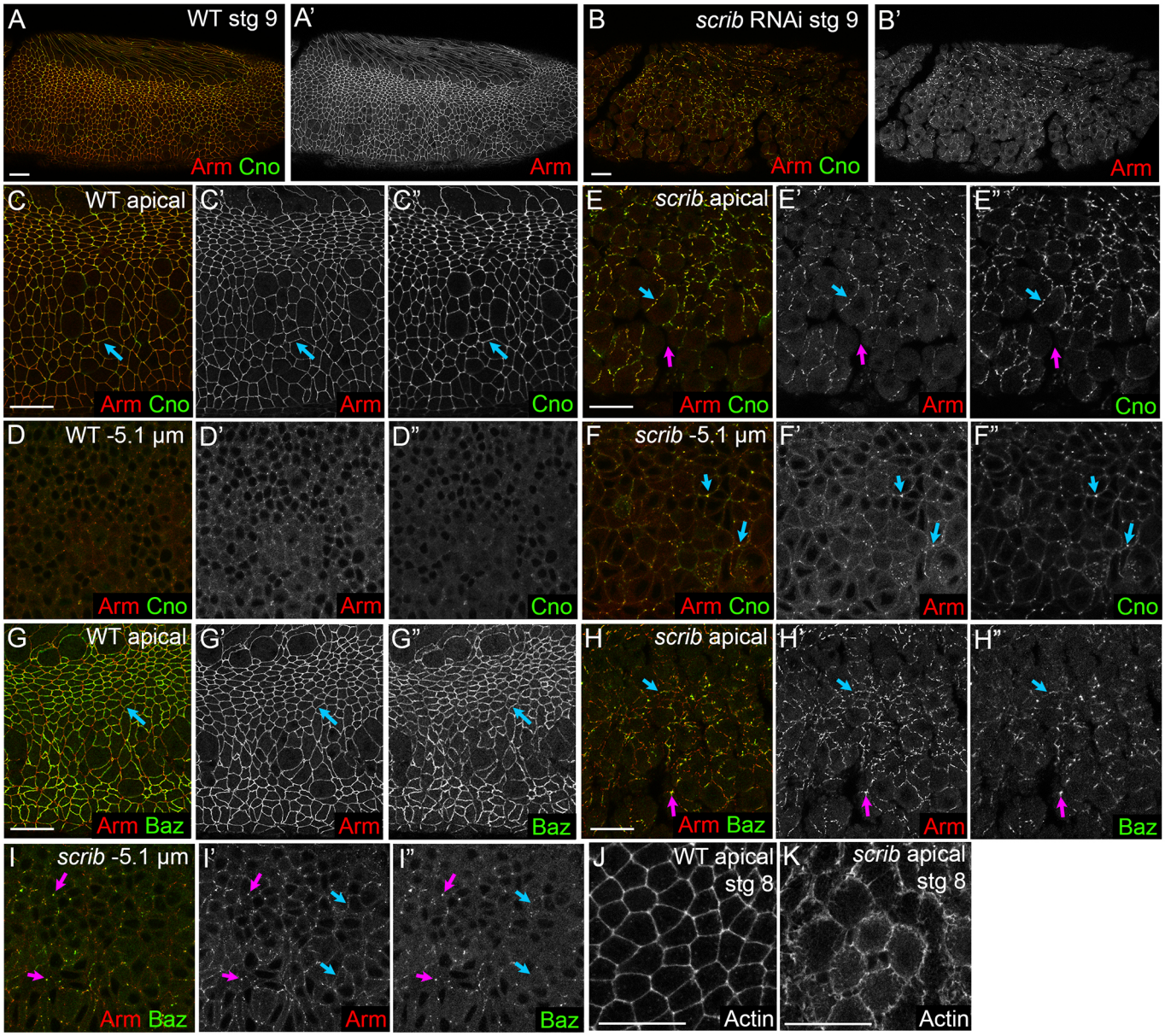

Fig. 6. After *scrib-RNAi*, cells rapidly lose epithelial character during gastrulation, and Arm and Cno colocalize in junctional fragments. (A-I″) Stage 9 *scrib-RNAi* embryos have fragmented AJs (A,A′ versus B,B′). In wild type, Arm, Cno and Baz form continuous belt junctions apically (C-C″,G-G″) with only occasional Arm puncta more basally (D-D″). (E-E″,F-F″,H-H″,I-I″) *scrib-RNAi.* Belt AJs fragment but Arm and Cno remain colocalized (E-E″, cyan arrows). Gaps form between cells (E-E″, magenta arrows) and junctional fragments appear basally (F-F″, cyan arrows). Baz disappears from belt junctions before Arm (H-I″, cyan arrows) and localizes to larger junctional fragments (H-I″, magenta arrows). (J) Wild-type stage 8. Apical actin lines cortex under AJs. (K) *scrib-RNAi.* Apical actin-based protrusions emerge. Scale bars: 20 µm.

endosome marker Rab11 are enriched in an apical compartment above nuclei (Pelissier et al., 2003; Fabrowski et al., 2013; Fig. S5A,C, white arrows); Rab5 also accumulates in small puncta laterally, and at the cellularization front (Fig. S5A,C, blue arrows), a place where DE-cad also accumulates after Arm knockdown (Harris and Peifer, 2004). However, *scrib-RNAi* does not eliminate apical enrichment of the Rab5 endocytic compartment (Fig. S5B,D, white arrows) nor does DE-cad accumulate there after *scrib-RNAi*. To directly test the hypothesis that Scrib/Dlg regulates AJ localization and organization via a Rab5-dependent mechanism, we expressed dominant-negative Rab5 (Rab5DN; Zhang et al., 2007; this led to highly penetrant embryonic lethality). Embryos maternally expressing Rab5DN completed cellularization normally and Cno remained tightly localized and correctly clustered in SAJs. However, SAJs were shifted downward along the apical-basal axis (Fig. S5E versus F) and mispositioning continued into early gastrulation (Fig. S5G versus H; quantified in K). This effect gradually disappeared as gastrulation proceeded, with Cno focusing apically as usual (Fig. S5I versus J). This unexpected phenotype is consistent with the idea that SAJ apical-basal polarization is regulated by at least two regulatory inputs – one determining precise SAJ localization along the apical-basal axis and others controlling supermolecular organization. It will be important to follow this up using Rab5 loss-of-function mutants or RNAi. One possibility is that the effect we observed is due to Rab5 reducing the size of the apical domain, as was suggested by Pelissier et al. (2003). However,

Development (2019) 146, dev180976. doi:10.1242/dev.180976

these data do not support the hypothesis that Scrib/Dlg act by promoting Rab5-regulated AJ trafficking, although this does not rule out a role for Scrib/Dlg more generally in trafficking of junctional proteins.

Scrib/Dlg regulates localization of the basolateral polarity protein Par-1 but Par-1 knockdown does not fully mimic knockdown of Scrib/Dlg

Par-1 is a basolateral polarity protein that helps restrict junctional and apical protein localization. Phosphorylation by Par-1 excludes Baz from the basolateral domain, and manipulating the balance of aPKC and Par-1 activity can re-position AJs (Bayraktar et al., 2006; Benton and St Johnston, 2003; Wang et al., 2012). However, the effects of Par-1 loss on DEcad and Baz localization during polarity establishment (Bayraktar et al., 2006) are largely rescued at gastrulation onset, owing to functional redundancy with dynein-based apical transport (McKinley and Harris, 2012). To investigate Par-1 in our own model, we first validated the Par-1 antibody and *par*-1 RNAi tool by immunofluorescence (Fig. S6A versus B,C versus D). During cellularization, Par-1 extends all along the membrane (Bayraktar et al., 2006; Fig. 7A), with highest cortical levels basally (Fig. 7B3, arrows in A indicate section planes) and gradually decreasing levels and less tight cortical localization as it extends apically to overlap SAJs and beyond (Fig. 7B2,B1). Par-1 is gradually cleared from the apical domain during early gastrulation, concentrating basolateral to AJs (Fig. S6A close-up, E). We first asked whether Scrib/Dlg regulate Par-1 localization during cellularization. After *dlg-RNAi*, cortical Par-1 levels were strongly reduced but not eliminated (Fig. 7A versus C). Interestingly, the strongest reduction of Par-1 cortical signal was in the basolateral region (Fig. 7B3 versus D3) rather than near the SAJs (Fig. 7B1 versus D1). To quantify this, we measured signal intensity at the basolateral membrane across the cell in cross-sections – in wild type, clear periodic peaks were observed at the cortex, and these were substantially reduced after *dlg-RNAi* (Fig. 7E; Fig. S1D; Fig. S6H). We assessed maximum peak height over the baseline across these transects and this revealed a significant drop in cortical intensity after *dlg-RNAi* (Fig. 7F). *scrib-RNAi* similarly reduced cortical Par-1 (Fig. S6F versus G; quantified in I,J).

We then examined whether *par-1-RNAi* recapitulated Scrib/Dlg knockdown, using a previously characterized shRNA. *par-1-RNAi* led to strong defects in blastoderm integrity due to partial loss of furrows in syncytial embryos, as previously reported (McKinley and Harris, 2012). This alone suggests Scrib/Dlg knockdown does not completely disable Par-1, as we do not observe this after Scrib/Dlg knockdown. We next examined effects of *par-1-RNAi* on AJs. Although *par-1-RNAi* altered polarity establishment, there were both differences and similarities between Par-1 and Scrib/Dlg knockdown. First, BJs were largely unaffected by *par-1-RNAi* (Fig. 7G,K,M versus I,L,N, cyan arrows, H versus J). However, the effects of Par-1 and Scrib knockdown on SAJs were quite similar. The normally tight enrichment of Arm in SAJs was lost (Fig. 7K′ versus L′,M′ versus N′, magenta arrows) – quantification revealed that the degree of loss of enrichment was similar to that seen after *scrib-RNAi* (Fig. 7Q versus 3H). Cno and Arm puncta also mislocalized up into the apical domain (Fig. 7K′ versus L′,M′ versus N′, yellow arrows), and the regular SAJ organization seen *en face* was also lost (Fig. 7O versus P), although this may reflect in part general disorganization of the apical membrane. In strong contrast to Scrib/Dlg knockdown, after *par-1-RNAi* there was partial rescue of AJ localization at gastrulation onset, with Arm and Cno cleared from the basolateral domain and AJs tightening (Fig. 7R versus S). This is consistent with Baz repolarization observed at this stage (McKinley and Harris, 2012). However, AJs in the dorsal and lateral ectoderm remained abnormally shifted basally (Fig. 7R versus S,T versus U, arrows), as was previously observed (Wang et al., 2012). Thus, Scrib/Dlg are required for Par-1 localization, and the partial overlap in phenotypes between *scrib-RNAi* and *par-1-RNAi* is consistent with the idea that altered Par-1 regulation may account in part for the effect of their loss. However, distinctions in phenotype suggest Par-1 regulation does not account for the full suite of polarity defects observed after Scrib/Dlg knockdown.

The leucine-rich repeats in Scrib are essential for polarity establishment and maintenance

Scrib and Dlg are both multi-domain scaffolding proteins with diverse sets of binding partners (Stephens et al., 2018). The overlap between Scrib/Dlg and SAJs is potentially consistent with a simple hypothesis – Scrib and/or Dlg act as scaffolds for AJ proteins during polarity establishment. Scrib contains an N-terminal leucine-rich repeat (LRR) and four C-terminal PDZ domains. Binding partners were identified for each domain, and mutational analyses begun to assess their individual roles. In *Drosophila*, *C. elegans* and mammals, the LRRs are required for cortical localization and are essential for almost all known functions (reviewed by Bonello and Peifer, 2019). To examine LRR function in this context, we used a particularly useful missense mutant in the LRRs of Scrib. In $scrib^{1}$, leucine 223 in the 10th LRR is changed to glutamine (Zeitler et al., 2004). This residue is conserved in all LAP proteins, and structural predictions suggest it is on the surface of the horseshoe-shaped LRR. Expression of a transgenic version in *Drosophila* suggest it encodes a stable protein, although it does not localize to the cortex. In previous assays, $scrib^{1}$ behaved as a null allele in most assays, including its effects on polarity in follicle cells, polarity maintenance and epithelial integrity in embryos, and loss of polarity and growth regulation in imaginal discs (though transheterozygous interactions with weak alleles suggest it may retain a small amount of function; Bilder et al., 2000; Bilder and Perrimon, 2000; Zeitler et al., 2004).

We thus generated females with germlines mutant for $scrib^{1}$ and crossed them to $scrib^{1}$ heterozygous males –50% of progeny are maternally and zygotically mutant, while 50% have a wild-type zygotic copy. The cuticle phenotype was as previously observed – maternal/zygotic mutants had the ‘scribbled’ cuticle phenotype (Fig. S3D,E). We confirmed by western blotting that the mutant protein was stable but accumulated at reduced levels (~50% wild type; Fig. S7A,B), and, consistent with work in imaginal discs (Zeitler et al., 2004), it did not localize to the cortex (Fig. S7C versus D). $scrib^{1}$ mutants recapitulated effects of *scrib-RNAi* on initial polarity establishment. AJ protein enrichment was lost in both SAJs (Fig. 8A,B versus E,F, cyan arrows) and BJs (Fig. 8A′,B versus E′,F, magenta arrows), and the normally tight Cno (Fig. 8A″,B′, cyan arrows) and Baz localization to SAJs (Fig. 8C′,D, cyan arrows) was reduced with puncta now found basolaterally (Fig. 8E″,F′,H, magenta arrows). Thus, the LRRs of Scrib are essential for its function in polarity establishment. As $scrib^{1}$ embryos gastrulated, polarity disruption was enhanced, with Cno and Arm spreading basolaterally at stage 7 (Fig. S7E versus G), and Baz puncta losing apical localization (Fig. S7F versus H). By stage 9, AJs were fragmented in $scrib^{1}$ (Fig. S7I versus J; Bilder and Perrimon, 2000). As we observed after *scrib-RNAi*, Arm and Cno colocalized in junctional fragments (Fig. S7K versus M, arrows), while Baz was restricted to brighter junctional fragments (Fig. S7L versus N, cyan versus magenta arrows). Thus, mutating this crucial residue in the LRRs essentially eliminated Scrib activity during

Development (2019) 146, dev180976. doi:10.1242/dev.180976

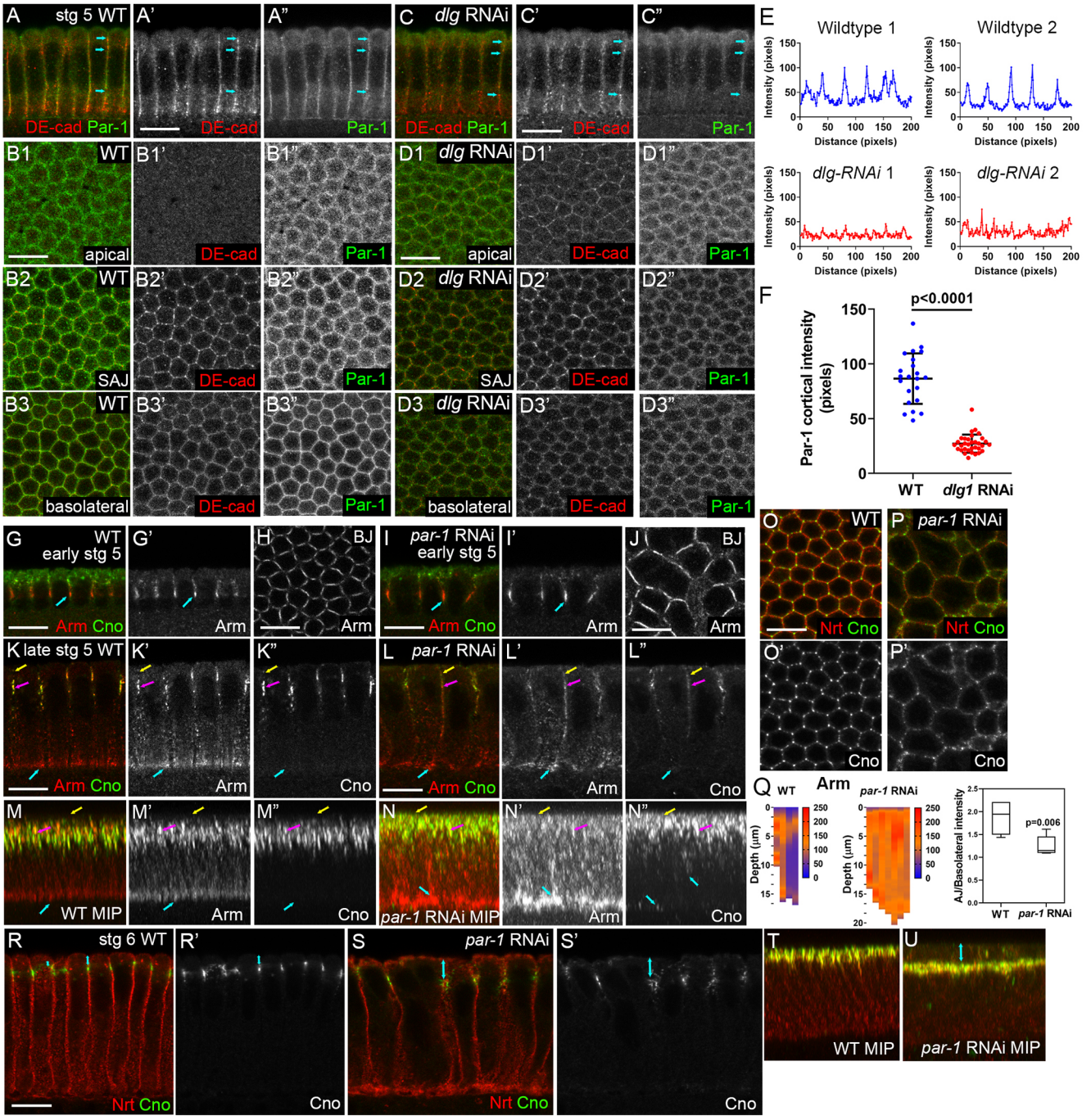

Fig. 7. Scrib/Dlg regulate Par-1 localization but Par-1 loss only partially mimics their phenotype. (A-A″,C-C″,G,G′,I,I′,K-K″,L-L″,R,R′,S,S′) Cross-sections. (M-M″,N-N″,R-U) MIPs. (B1-D3″,H,J,O-P′) *En face* sections at indicated position. (A-D3″) In wild type (A-B3″), Par-1 localizes in a gradient at the cortex, with highest levels basolaterally. Arrows in A-A″ indicate positions of sections in B1-B3″. After *dlg-RNAi* (C-D3″) cortical Par-1 is reduced. (E,F) Signal intensity at basolateral membrane in cross-sections. (E) In wild type, clear periodic peaks were observed at the cortex; these were significantly reduced after *dlg-RNAi*. (F) Quantification of maximum peak height over baseline (data are mean±s.d. with individual data points shown). (G-P′) *par-1-RNAi* reduces Arm enrichment in SAJs during cellularization (K,K′,M,M′ versus L,L′,N,N′, magenta arrows) but does not eliminate Arm enrichment in BJs (G,G′,K,K′,M,M′ versus I,I′,L,L′,N,N′, cyan arrows; H versus J). Cno is less affected, although it expands apically (K-K″,M-M″ versus L-L″,N-N″, yellow arrows) and basolaterally (M″ versus N″, cyan arrows) and TCJ enrichment is reduced (O-P′). (Q) *par1-RNAi* significantly reduces Arm enrichment in SAJs. Pixel plots along apical-basal axis and quantification of Arm enrichment in SAJs versus basolateral domain (box and whisker plot; data are median, upper and lower quartile limits, and range). (R-U) Gastrulation onset. Arm and Cno refocus into belt AJs after *par-1-RNAi* but AJs localize more basally (R,R′ versus S,S′, T versus U, arrows). Scale bars: 10 µm.

cellularization and gastrulation, consistent with what was observed in other tissues (Bilder et al., 2000; Bilder and Perrimon, 2000; Zeitler et al., 2004). As we observed after *scrib-RNAi*, there was partial rescue of junctional polarity much later (stage 13; Fig. S3J).

The PDZ domains of Scrib are required to focus SAJs apically during polarity establishment, but become dispensable for AJs after gastrulation

Intriguingly, while LRR mutations largely or completely inactivate Scrib, the PDZs are not essential for all functions. *scrib*^{4}, which

Development (2019) 146, dev180976. doi:10.1242/dev.180976

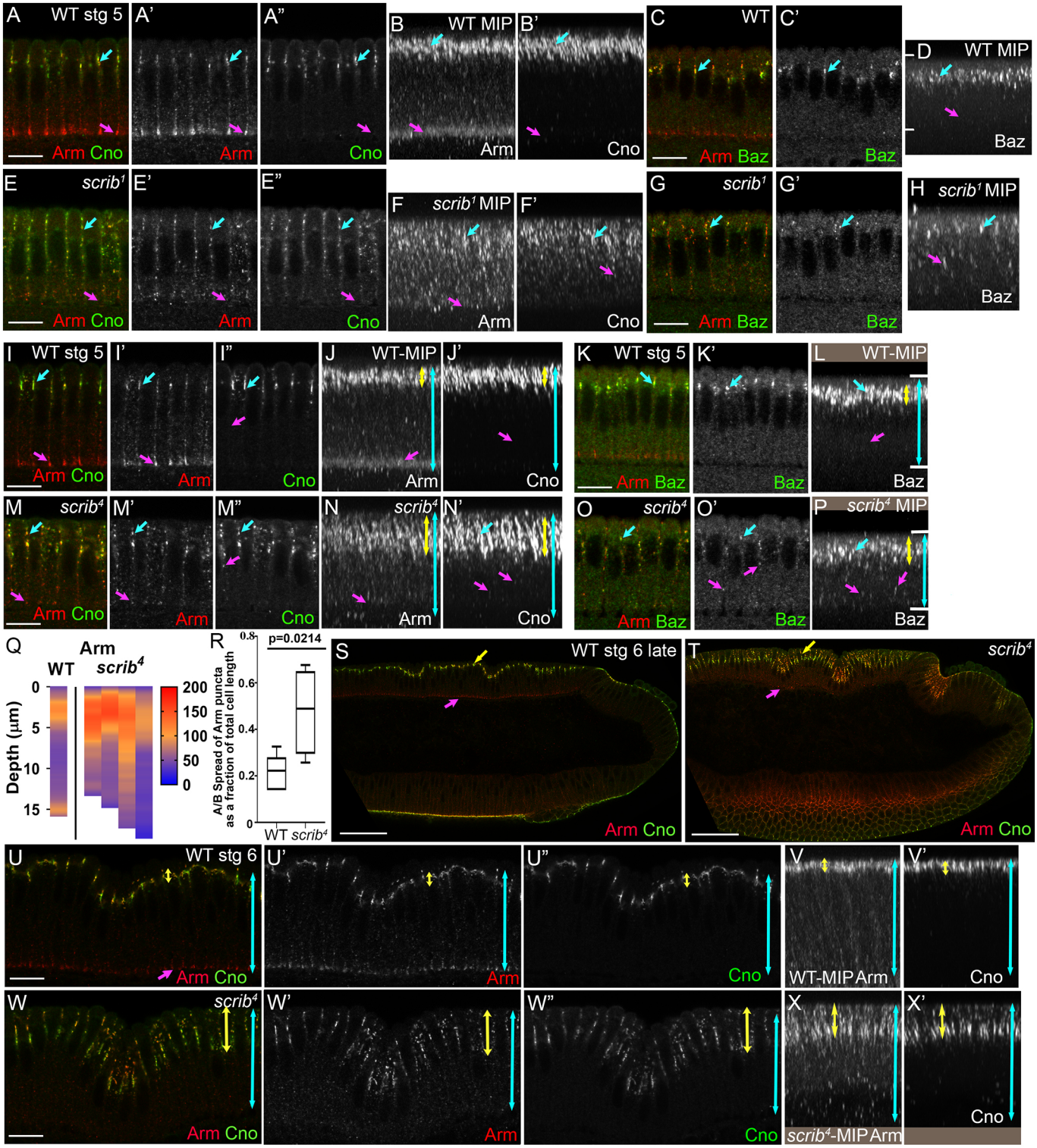

Fig. 8. The LRR domain of Scrib is essential for polarity establishment, while the PDZ domains of Scrib are important for polarity during cellularization but not after gastrulation. (A-A″,C,C′,E-E″,G,G′,I-I″,K,K′,M-M″,O,O′,S-U″,W-W″) Cross-sections. (B,B′,D,F,F′,H,J,J′,L,N,N′,P,V,V′,X,X′) MIPs. (A-R) Cellularization. (A-H) Wild type versus *scrib*^{1}. Arm enrichment in apical SAJs and BJs (A′,B, cyan and magenta arrows, respectively) is lost in *scrib*^{1} (E′,F). Cno positioning and assembly into cables at SAJs (A″,B′) is disrupted in *scrib*^{1}, although some apical enrichment remains (E″,F′). Tight apical restriction of Baz in wild type (C-D) is relaxed in *scrib*^{1} (G-H). (I-X′) Wild type versus *scrib*^{4}. (I-R) Cellularization. In *scrib*^{4}, normally tight apical localization of Arm and Cno to SAJs during cellularization spreads over an expanded area (I-J′ versus M-N′, yellow arrows), Arm enrichment in BJs is lost (J versus N, magenta arrows), and Cno puncta appear basally (J′ versus N′, magenta arrows). Baz puncta, which are normally restricted to SAJs (K-L, cyan arrows), are seen basally (K-L versus O-P, magenta arrows). (Q) Quantification of Arm displacement by heat maps. (R) Quantification of the fraction of cell length occupied by normal or expanded SAJs (box and whisker plot; data are median, upper and lower quartile limits, and range; methodology in Fig. S1E). (S-X′) Gastrulation onset. In wild type, Arm and Cno tighten apically both dorsally (S,U-U″, yellow arrows) and laterally (V,V′, yellow arrow). Arm and Cno distribute over a broader region in *scrib*^{4} (U-U″ versus W-W″, V,V′ versus X,X′, yellow arrows). Scale bars: 50 µm in S,T; 10 µm in A-P,U-X′.

Development (2019) 146, dev180976. doi:10.1242/dev.180976

encodes a truncated Scrib lacking all four PDZs, has been very informative. This mutant protein accumulates as a stable protein when expressed from a transgene (Zeitler et al., 2004), and we verified that this transgenic protein can accumulate in early embryos (Fig. S7T; it is not recognized by existing anti-Scrib antibodies). *scrib*^{4} rescues apical-basal polarity in later embryos and imaginal discs, but does not rescue SJ assembly or fully rescue growth regulation in imaginal discs (Zeitler et al., 2004). Its embryonic cuticle phenotype illustrates this – while the cuticle is reduced to fragments in *scrib*-null mutants, it remains intact in *scrib*^{4} mutants, although head involution and dorsal closure are disrupted (Fig. S3F,H).

Use of *scrib*^{4} allowed us to selectively disrupt a different subset of protein interactions with Scrib and examine their effects. Consistent with previous reports, *scrib*^{4} maternal/zygotic mutants retained significant ectodermal integrity at the end of gastrulation (Fig. S7Q; Zeitler et al., 2004). We next looked during cellularization, to examine whether polarity establishment proceeded normally. To our surprise, *scrib*^{4} embryos had defects in SAJ positioning during cellularization, although these differed from those seen after *scrib-RNAi* or in *scrib*^{1} mutants. In wild type, Arm is tightly enriched in both apical SAJs and BJs (Fig. 8I,J, cyan and magenta arrows, respectively), with lower levels along the basolateral membranes, and Cno (Fig. 8I″,J′) and Baz (Fig. 8K′,L) are tightly restricted to SAJs. SAJs occupy roughly the apical 20% of the cell length (quantified in Fig. 8Q,R). In *scrib*^{4}, SAJ-enriched Arm and Cno expanded apically and basolaterally (Fig. 8I versus M,J versus N, yellow arrows, J′ versus N′, magenta arrows; Arm quantified in Q, R), such that they now spanned more than 40% of the cell length (see Fig. S1E for methodology). This differed from total loss of apical enrichment of Arm seen in *scrib*^{1} mutants (Fig. 8F). Arm enrichment at basal junctions was also lost in *scrib*^{4} (Fig. 8J versus N, magenta arrows). Baz was still enriched at the SAJ level (Fig. 8L versus P, cyan arrows), but Baz puncta were also seen more basally in *scrib*^{4} mutants (Fig. 8L versus P, magenta arrows). These data are consistent with a role for the PDZ domains of Scrib in initial polarity establishment, but the AJ defects were distinct from those of *scrib*^{1} (Fig. 8A-H) or *scrib-RNAi*. It will be important in the future to examine in detail the localization and accumulation level of a Scrib protein lacking the PDZs – analysis in imaginal discs suggests that this protein can localize to the cortex but may be defective in polarized accumulation (Zeitler et al., 2004).

We then followed *scrib*^{4} mutants to see when and how polarity was re-established. In wild type, AJs move apically and become even more focused by late stage 6 (Fig. 8S,U,V, yellow arrows), although some Arm remains in BJs (Fig. 8S,U, magenta arrows). In contrast, in *scrib*^{4}mutants, rather than focusing, SAJs, as marked by both Arm and Cno, continued to be substantially broadened at gastrulation onset – both extended further basolaterally in both the dorsal (Fig. 8U versus W, yellow arrows) and lateral epidermis (Fig. 8V versus X, yellow arrows). The transition from SAJs to belt AJs in *scrib*^{4} was also delayed (Fig. S7O versus P). Remarkably, however, AJ repolarization was complete by the end of germband extension (Fig. S7Q, *z*-stack reconstructions R versus S), unlike what we observed after *scrib-RNAi*. Thus, the PDZ domains of Scrib are required for many aspects of proper polarity establishment, but PDZ domain-independent mechanisms appear during gastrulation and restore polarity.

BioID suggests mammalian Scribble and Afadin are also in close proximity in MDCK cells

The data above suggest that Scrib localizes in a way that overlaps the AJ during polarity establishment and is important for AJ positioning. As detailed in the Introduction, previous data have suggested a role for Scrib in cell-cell adhesion in MDCK cells. Strikingly, while our manuscript was under review, the Troyanovsky group found that the three mammalian LAP proteins Scribble, Erbin and Lano play redundant roles in epithelial polarity in cultured mammalian cells (Choi et al., 2019). We wondered whether the overlap in localization observed in early fly embryos was also a feature of mammalian cells. The BioID method, in which a promiscuous biotin ligase (BirA-R118G) is added to a protein of interest, provides a means of assessing whether two proteins are in close proximity in living cells (most estimates are tens of nanometers; Roux et al., 2012; Sears et al., 2019). We had generated for other experiments doxycycline-inducible versions of mammalian Afadin, the Cno homolog, tagged with BirA at either the N- or C-terminus. Using the well-characterized epithelial cell line MDCK, we generated stable cell lines expressing each fusion, and generated a control cell line expressing BirA alone. In both experimental cell lines, Afadin and Scribble overlapped in localization at cell-cell junctions, as assessed by immunofluorescence (Fig. 9A-D; we used two different pairs of anti-Scribble and Afadin antibodies, as well as antibodies to the Myc-epitope to confirm this), but they do not strictly colocalize, reminiscent of what we observed in *Drosophila*. Cells were induced to express the fusion proteins, incubated with biotin for ∼28 h and biotin-labelled proteins were then pulled down using streptavidin-coated beads. Input, unbound and bound fractions were probed for Afadin and Scrib. Afadin pulldown in cells expressing either the N-terminal or C-terminal BirA fusions was highly effective, as visualized by blotting with antibodies to Afadin (Fig. 9E, top row) or to the Myc-epitope tag (Fig. 9E, second and third rows), presumably owing to self-biotinylation. However, Afadin was not pulled down in the negative control cell line expressing BirA alone. Similarly, BirA-Myc expressed alone was also effectively self-biotinylated and pulled down with streptavidin (Fig. 9E, fourth row). The negative control, tubulin, was not pulled down in any of the cell lines (Fig. 9E, bottom row). Strikingly, Scrib was pulled down from cells expressing either BirA-Afadin or Afadin-BirA, but not in cells expressing BirA alone (Fig. 9E, fifth and sixth rows; quantified in F). These data are consistent with the overlap in localization of Scrib and Canoe/Afadin being a conserved feature of animal epithelia.

DISCUSSION

Identifying the earliest symmetry-breaking events that initially position AJs, thereby setting the boundary between apical and basolateral domains, is a key aspect of understanding how polarity is established. Here, we report that Scrib/Dlg, which are best known for their roles as basolateral determinants during polarity maintenance, play a separate and surprising role in organizing AJs during polarity establishment, positioning them near the top of the polarity network.

Master directors of junction supermolecular organization

Scrib and Dlg are multidomain proteins with many partners, allowing them to serve diverse biological functions, from synaptogenesis to oriented cell division. Our data reveal that they play distinct roles during polarity establishment and polarity maintenance, likely engaging very different sets of binding partners. This is supported by the evolving localization pattern of Scrib/Dlg on the plasma membrane, with sequential colocalization with and roles in positioning AJ versus SJ proteins, suggesting the capacity to engage with and position distinct junctional and polarity proteins. Our analyses also begin to dissect the underlying molecular basis. The PDZ domains of Scrib are important for the precision of initial polarity establishment but are redundant with

Development (2019) 146, dev180976. doi:10.1242/dev.180976

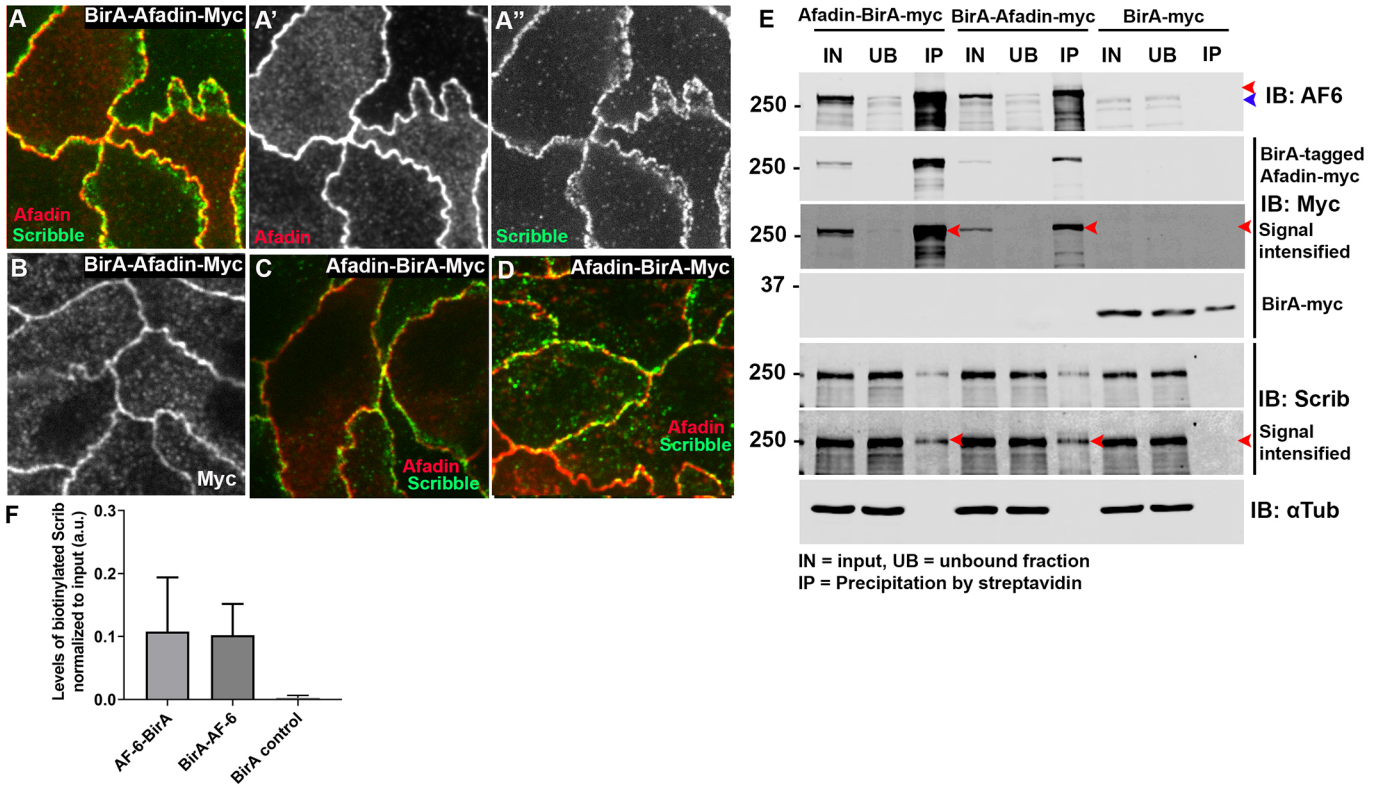

Fig. 9. BioID reveals that mammalian Scribble and the Canoe homolog Afadin are in close proximity in MDCK cells. (A-D) MDCK cells transfected with Afadin/BirA constructs and stained for Afadin, Scribble or Myc epitope. Both BirA-Afadin-Myc (A,B) and Afadin-BirA-Myc (C,D) localize cortically and overlap with Scribble. (C,D) Different Afadin and Scribble antibodies. (E) MDCK cells, input (IN), unbound (UB) and streptavidin-bound (IP) fractions probed for Afadin and Scrib. As expected, Afadin pulldown by streptavidin in cells expressing either the N-terminal or C-terminal BirA fusions was highly effective, as visualized by blotting with antibodies to Afadin (top row; arrowheads indicate endogenous and tagged Afadin) or Myc epitope tag (second and third rows, arrowheads indicate BirA-tagged Afadin), presumably owing to self-biotinylation. Neither was pulled down in the negative control cell line expressing BirA alone. Similarly, BirA-Myc expressed alone was effectively biotinylated and pulled down with steptavidin (fourth row). The negative control, tubulin, was not pulled down in any of the cell lines (bottom row). Strikingly, Scrib was pulled down from cells expressing either BirA-Afadin or Afadin-BirA, but not in cells expressing BirA alone (fifth and sixth rows; arrowheads indicate presence or absence of Scrib in pulldown). (F) Quantification of Scrib pulldown by three BirA fusions (data are mean±s.d.).

other mechanisms for polarity maintenance after gastrulation, although they regulate SJ positioning.

AJs play a key role at the boundary between apical and basolateral domains, and building a functional AJ is a multistep process. This includes assembling a stable core cadherin-catenin complex, positioning it and supermolecular assembly. Assembly of the core complex into small puncta occurs before cellularization. As cellularization proceeds, these are captured at the apicolateral interface in a process requiring Baz, Cno and an intact actin cytoskeleton, where they coalesce into SAJs, with ∼1500 cadherin-catenin complexes and 200 Baz proteins (McGill et al., 2009). Cadherin-catenin complexes form independently of either Baz or Cno, but AJ positioning and full supermolecular assembly depend on both. We found that Scrib/Dlg are also key for AJ apicolateral retention and supermolecular assembly, although Arm and Cno remain associated in misplaced puncta, and thus core AJ complexes remain intact. Furthermore, a second junctional complex that arises during polarity establishment, the BJ, also requires Scrib/Dlg for its supermolecular organization. Unlike AJs, BJ organization is not dependent on other polarity determinants, including Cno, Rap1 or Par-1. It will be of interest to examine whether Scrib/Dlg act via known regulators of cadherin clustering, considering both intrinsic (e.g. cis- and trans-interactions of cadherins) and extrinsic factors (e.g. local actin regulation, endocytosis; Truong Quang et al., 2013). It is also important to note that our analyses generally use heat fixation, which emphasizes the most stably associated junctional proteins and reduces the diffuse cytoplasmic pool – it may be that Scrib/Dlg normally stabilize junctional localization of proteins such as Baz, rather than being absolutely essential for their recruitment there. We also note that others have reported a potential role for Dlg in 'plasma membrane formation' during cellularization (Lee et al., 2003) – we did not observe any effects on cellularization per se in our *dlg* knockdown conditions, nor have defects been reported in earlier examinations of *dlg* maternal/zygotic mutants (Bilder et al., 2000; Blankenship et al., 2007)

The Scrib/Dlg module shapes polarity establishment and maintenance via multiple mechanisms

Our ultimate goal is to define molecular mechanisms underlying polarity establishment. Our new data place Scrib/Dlg in a crucial position near the top of the network, but also suggest they act via multiple effectors. Perhaps the strongest evidence for multiple roles with distinct effectors comes from analysis of *scrib*^{4}. Our data reveal that supermolecular organization of both SAJs and BJ must involve interactions with specific partners via the PDZ domains – one speculative possibility is that these include core AJ proteins, as β-catenin can co-immunoprecipitate with Scribble and interacts with PDZ domains 1 and 4 (Ivarsson et al., 2014; Zhang et al., 2006). Testing this idea will be an important future direction. The initial role of Scrib may also involve modulating Par-1. During cellularization, Scrib/Dlg and Par-1 localize in 'inverse gradients': Scrib and Dlg enriched at the SAJ level, and Par-1 with higher

Development (2019) 146, dev180976. doi:10.1242/dev.180976

cortical intensity basolaterally. Scrib/Dlg play a role in effective membrane recruitment of Par-1 at this stage. The qualitative and quantitative effects of *par-1-RNAi* on SAJ protein localization during cellularization are similar to those of *scrib-RNAi*, although they also differed in important ways – *par-1-RNAi* did not disrupt BJs and its effects on polarity were partially rescued as gastrulation began. It will be interesting to test whether and to what degree overexpressing Par-1 or targeting it to the membrane can rescue loss of Scrib/Dlg. These data are consistent with the idea that regulating Par-1 may be one of several mechanisms by which Scrib/Dlg act.

Scrib then plays a second PDZ-independent role as gastrulation begins, ensuring focusing of cadherin-catenin complexes and Baz into apical belt AJs. This requires the N-terminal LRRs, as was observed in other times and places, but not the PDZs. Positioning Baz at this stage involves at least two inputs that are redundant with one another, one via Par-1 and one via an apical transport mechanism (McKinley and Harris, 2012). One speculative possibility is that Scrib/Dlg also regulate protein trafficking, a role they have in other contexts. However, disrupting Scrib/Dlg function has very different consequences from disrupting Rab5-dependent trafficking using a dominant negative, suggesting they are not likely to act by activating Rab5. aPKC also provides important cues at this stage – perhaps Scrib/Dlg regulate aPKC localization or function. It will be important to further explore the nature of this second role.

As outlined in the Introduction, work in cultured mammalian cells supports a role for Scribble in cadherin-based adhesion and apical-basal polarity, suggesting that this is a conserved function. However, effects of Scribble knockout in the mouse suggested it is not crucial in all tissues. An important paper appeared while this work was under review that may help resolve this. Mammals have three LAP family proteins – Scrib, Erbin and Lano – raising the possibility of functional overlap. Consistent with this, triple knockdown of all three proteins in DLD1 cells led to much more substantial defects in apical junctional assembly and polarity (Choi et al., 2019). It will be of interest to compare mechanisms.

Defining the polarity establishment network and identifying the ultimate upstream cue for polarity establishment

Our initial goal more than a decade ago was to define roles of AJs in polarity establishment. However, it rapidly became apparent AJs are not at the top of the hierarchy. Cno, Rap1 and Baz act upstream of AJ positioning and supermolecular assembly. Our new data and earlier work also suggest that polarity establishment is not a linear pathway, but instead involves a network of interactions with multiple inputs and also feedback regulation. The data here uncover a new crucial link in the network, revealing a key role for Scrib/Dlg in regulating AJ positioning and assembly. However, they also emphasize that the process is not a simple linear pathway, and raise new questions. Loss of Scrib or Dlg almost completely disrupts AJs during cellularization. However, effects on Baz and Cno, both of which also localize to nascent AJs, are less complete – their supermolecular assembly is affected, but they are largely retained in the apical half of the membrane. This suggests that there are multiple parallel inputs into AJ assembly, an idea also supported by the relatively uniform distribution of Scrib/Dlg at the level of nascent AJs, as opposed to the punctate assembly of spot AJ proteins. The role of Scrib/Dlg in both BJs and SAJs, which have distinct inputs and a very different supermolecular architecture, also support the idea that Scrib/Dlg are one of several inputs. Finally, Rap1 and Baz are required for proper apical enrichment of Dlg near SAJs during cellularization, while assembly of AJs is not, suggesting a non-linear network with feedback regulation. A similar model with multiple upstream inputs and complex interdependencies was proposed for polarization of the follicle cell epithelium, in which AJ position requires inputs from Dlg, Arm/β-catenin and Baz/Par3 (Franz and Reichmann, 2010).

The ultimate polarizing cue during syncytial development is the oocyte membrane, which then directs cytoskeletal polarization. Cytoskeletal cues regulate Cno localization. Although our data rule out a role for Scrib/Dlg in establishing basic cytoskeletal polarity, they do not rule out more subtle roles, for example, in localizing a special 'type' of actin cytoskeleton in the apical domain. Retention of Cno at the membrane after Scrib/Dlg knockdown suggests that basal Rap1 activity remains intact. Changes to early Par-1 and Baz cortical localization with loss of Scrib/Dlg, also raise the possibility that lipid-based regulation is impaired (Kullmann and Krahn, 2018; McKinley et al., 2012). At this time, we do not know what cues regulate Scrib/Dlg apical enrichment but AJs do not appear to direct this, nor are they essential for polarizing Cno or Baz, which do play a role in Dlg apical enrichment. Continued characterization of the full protein network and molecular mechanisms governing polarity establishment will keep the field busy for years to come.

MATERIALS AND METHODS

Fly genetics

Fly stocks used in this study are listed in Table S1. Mutations are described at FlyBase (flybase.org). Wild type was yellow white. All experiments were carried out at 25°C, with the exception of driving *arm* RNAi, which was carried out at 27°C. Knockdown by RNAi was achieved by crossing double copy maternal GAL4 females (Staller et al., 2013) with males carrying the UAS hairpin construct. Female progeny were then crossed back to males carrying the UAS hairpin construct. For *scrib* RNAi, most experiments were carried out with the valium 22 line, but key conclusions were verified with the valium 20 line. For driving *arm* RNAi expression, the GAL4 was provided by the males (Ni et al., 2011). Maternal expression of dominant-negative Rab5 was carried out by crossing female double maternal GAL4 flies with males carrying UAS-YFP.Rab5.S43N. To create germline clones, $scrib^{1}$ or $scrib^{4}$ females were crossed with males carrying hsFLP;;FRT82B ovoD1. Wandering larvae were heat shocked for 2 h in a 37°C water bath on 2 consecutive days.

Immunostaining (embryos)

Staining for Nrt, Arm, Cno, Baz, Scrib, Rab5 and Zip was performed using the heat-fix method. Dechorionated embryos were fixed in boiling Triton salt solution (0.03% Triton X-100, 68 mM NaCl) for 10 s followed by fast cooling on ice and devitellinized by vigorous shaking in 1:1 heptane:methanol. Embryos were stored in 95% methanol/5% EGTA for at least 48 h at −20°C prior to staining. For staining all other antigens, embryos were fixed for 20 min with 9% formaldehyde and devitellinized in 1:1 heptane:methanol, except for staining with phalloidin, where embryos were devitellinized in 1:1 heptane:90% ethanol. Prior to staining, embryos were washed with 0.1% Tween-20 in PBS (heat-fixed embryos) or 0.1% Triton X-100 in PBS (formaldehyde-fixed embryos), and blocked in 1% normal goat serum in PBS-T for 1 h. Primary and secondary antibody dilutions are listed in Table S1.

Image acquisition, manipulation and quantification

Fixed embryos were mounted in Aqua-poly/Mount and imaged on a confocal laser-scanning microscope (LSM 880;40×/NA 1.3 Plan-Apochromat oil objective; Zeiss). Images were processed using ZEN 2009 software. Photoshop CS6 (Adobe) was used to adjust input levels so that the signal spanned the entire output grayscale and to adjust brightness and contrast. Maximum intensity projections (MIPs) were generated by acquiring *z*-stacks through the embryo with a 0.3 µm step size and digital zoom of two. ZEN 2009 software was used to crop stacks to 250×250 pixels along the *xy*-axis and to project *xyz*-stacks along the *y*-axis as previously described (Choi et al., 2013). The apical-basal position of puncta was determined from MIPs using ImageJ (NIH). Projections were rotated

90° counterclockwise and analyzed using the Plot Profile function in ImageJ to generate values of average fluorescence intensity along the apical-basal axis. These data were displayed as heat maps, illustrating intensity along the apical-basal axis with a color gradient. Graphs and accompanying heat maps were generated using GraphPad Prism 8.0. A complete description of all other quantification can be found in Fig. S1. Statistical analysis was performed using unpaired, two-tailed *t*-tests. A full list of *n*-values is presented in Table S2.

Cuticle preparation

Cuticle preparation was performed according to Wieschaus and Nusslein-Volhard (Wieschaus and Nüsslein-Volhard 1986).

Immunoblotting

Knockdown efficiency by RNAi was evaluated by western blotting. Embryo lysates were prepared by grinding dechorionated embryos in ice-cold lysis buffer [1% NP-40, 0.5% Na deoxycholate, 0.1% SDS, 50 mM Tris (pH 8), 300 mM NaCl, 1.0 mM DTT and Halt protease and phosphatase inhibitor cocktail (Thermo Fisher Scientific)]. Lysates were cleared at 16,000 ***g***, and protein concentration determined using the Bio-Rad Protein Assay Dye (Bio-Rad). Lysates were resolved by 8% SDS-PAGE, transferred to nitrocellulose filters and blocked for 1 h in 10% dry milk powder in PBS-T (0.1% Tween-20 in PBS). Membranes were incubated in primary antibody for 2 h (see Table S1 for antibody concentrations); washed four times for 5 min each in PBS-T and incubated with IRDye-coupled secondary antibodies for 45 min. Signal was detected using the Odyssey infrared imaging system (LI-COR Biosciences). Band densitometry was performed using ImageStudio software version 4.0.21 (LI-COR Biosciences).

Stable expression of BirA-Afadin in mammalian epithelial cell culture

The rat Afadin coding sequence was subcloned into pTRE2hyg-BirA-myc, an inducible mammalian expression vector for BioID (Van Itallie et al., 2013) at the N- (pTRE2hyg-Afadin-BirA-myc) or C-terminus of the BirA gene (pTRE2hyg-BirA-Afadin-myc) using a Gibson assembly reaction (New England Biolabs). Subconfluent MDCK T23 cells were transfected with N- or C-terminal tagged BioID plasmids and selected for the stable clones using hygromycin as a selective drug. The stable clones were verified by western blot and immunostaining for Afadin and Myc tag. Cells expressing BirA-Afadin were cultured in DMEM media containing 1 g/l glucose, 10% fetal bovine serum, 15 mM HEPES (pH 7.4) and 50 ng/ml doxycycline. For plating cells in polycarbonate Transwell inserts (Thermo Fisher Scientific), doxycycline was removed to induce the expression of transgenes.

Immunostaining (cell culture)

Cells were cultured for 7 days in the Transwells without doxycycline to express BirA-Afadin and fixed in ice-cold ethanol for 1 h at −20°C. After three washes with PBS, the samples were incubated with blocking buffer (10% FBS in PBS) for 1 h at room temperature. Subsequently, the inserts were incubated with primary antibodies diluted in blocking buffer. Rabbit anti-Afadin and mouse anti-Scribble, or rabbit anti-Scribble and mouse anti-Myc antibodies were used for co-staining. Following three washes with wash buffer (1% FBS in PBS), the cells were incubated with the Alexa-conjugated secondary antibodies along with Hoechst 33343 to stain DNA. After three washes with wash buffer, the insert membrane was cropped out, mounted on a microscope slide with Prolong Diamond antifade mountant (Thermo Fisher Scientific) and cured before imaging.

Purification of biotinylated proteins for immunoblotting

MDCK cells were those used by Choi et al. (2016), and were authenticated and tested for contamination. MDCK cells stably expressing BirA transgenes were cultured without doxycycline for 5 days, following which cells were treated with 50 µM biotin for 27-28 h. To prepare lysates, cells were washed three times with ice-cold PBS and scraped into lysis buffer [1% NP-40, 0.5% deoxycholate, 0.2% SDS, 50 mM Tris (pH 8), 150 mM NaCl, 2 mM EDTA, supplemented with protease/phosphatase inhibitor]. Lysates were snap frozen on dry ice prior to storing at −80°C. To capture biotinylated proteins, lysates were thawed at 4°C, sonicated (amplitude 50%, 10 strokes performed manually) and incubated on ice for 15 min. Lysates were then spun at 15,000 ***g*** for 15 min and the protein concentration of supernatant determined using BioRad Protein Assay Dye. Equal concentrations of sample were added to pre-washed Dynabeads (MyOne Streptavidin C1) and incubated with nutation overnight at 4°C. After removing the unbound sample, beads were washed twice with buffer 1 (2% SDS) for 10 min, once with buffer 2 [0.1% deoxycholate, 1% Triton X-100, 500 mM NaCl, 1 mM EDTA and 50 mM Hepes (pH 8)] for 10 min, once with buffer 3 [0.5% deoxycholate, 0.5% NP-40, 250 mM NaCl, 1 mM EDTA and 10 mM Tris (pH 8)] for 10 min and twice with buffer 4 [50 mM NaCl and 50 mM Tris (pH 7.4)] for 10 min. To elute bound proteins, 40 µl of biotin-saturated 2× SDS sample buffer (50 µm biotin) was added to the beads and boiled for 10 min. For SDS-PAGE electrophoresis, 15 µl of eluate was run out on an 8% acrylamide gel, transferred overnight to a nitrocellulose membrane and probed with the following antibodies: anti-Scribble (MAB1820), anti-Afadin (A0224) and anti-Myc (SC-40).

Acknowledgements

We thank David Bilder and Mark Khoury for the Scribble antibody, *scribble* mutant stocks, advice in generating maternal-zygotic mutants and helpful discussions; Jocelyn McDonald, Jeffrey Thomas, the Bloomington Drosophila Stock Center, the Transgenic RNAi Project (TRiP) and the Developmental Studies Hybridoma Bank for reagents; Tony Perdue of the Biology Imaging Center; Clara Williams, Jonathan Deliberty and Ian Windham for technical assistance; John Poulton for reagents and thoughtful discussion; Scott Williams, Peifer lab members and the three reviewers for helpful advice and comments; and Bing He for helpful discussions.

Competing interests

The authors declare no competing or financial interests.

Author contributions

Conceptualization: M.P., T.T.B.; Methodology: M.P., T.T.B.; Investigation: M.P., W.C., T.T.B.; Writing - original draft: M.P., W.C., T.T.B.; Writing - review & editing: M.P., W.C., T.T.B.; Supervision: M.P., T.T.B.; Funding acquisition: M.P.

Funding

This work was supported by National Institutes of Health (R35 GM118096 to M.P.). T.T.B. was supported in part by a Sir Keith Murdoch Fellowship from the American Australian Association. Deposited in PMC for release after 12 months.

Supplementary information

Supplementary information available online at
http://dev.biologists.org/lookup/doi/10.1242/dev.180976.supplemental

References

Awadia, S., Huq, F., Arnold, T. R., Goicoechea, S. M., Sun, Y. J., Hou, T., Kreider-Letterman, G., Massimi, P., Banks, L., Fuentes, E. J. et al. (2019). SGEF forms a complex with Scribble and Dlg1 and regulates epithelial junctions and contractility. *J. Cell Biol.* **218**, 2699-2725. doi:10.1083/jcb.201811114

Baumgartner, S., Littleton, J. T., Broadie, K., Bhat, M. A., Harbecke, R., Lengyel, J. A., Chiquet-Ehrismann, R., Prokop, A. and Bellen, H. J. (1996). A Drosophila neurexin is required for septate junction and blood-nerve barrier formation and function. *Cell* **87**, 1059-1068. doi:10.1016/S0092-8674(00)81800-0

Bayraktar, J., Zygmunt, D. and Carthew, R. W. (2006). Par-1 kinase establishes cell polarity and functions in Notch signaling in the Drosophila embryo. *J. Cell Sci.* **119**, 711-721. doi:10.1242/jcs.02789

Bazellieres, E., Aksenova, V., Barthelemy-Requin, M., Massey-Harroche, D. and Le Bivic, A. (2018). Role of the Crumbs proteins in ciliogenesis, cell migration and actin organization. *Semin. Cell Dev. Biol.* **81**, 13-20. doi:10.1016/j.semcdb.2017.10.018

Benton, R. and St Johnston, D. (2003). Drosophila PAR-1 and 14-3-3 inhibit Bazooka/PAR-3 to establish complementary cortical domains in polarized cells. *Cell* **115**, 691-704. doi:10.1016/S0092-8674(03)00938-3

Bilder, D. and Perrimon, N. (2000). Localization of apical epithelial determinants by the basolateral PDZ protein Scribble. *Nature* **403**, 676-680. doi:10.1038/35001108

Bilder, D., Li, M. and Perrimon, N. (2000). Cooperative regulation of cell polarity and growth by *Drosophila* tumor suppressors. *Science* **289**, 113-116. doi:10.1126/science.289.5476.113

Bilder, D., Schober, M. and Perrimon, N. (2003). Integrated activity of PDZ protein complexes regulates epithelial polarity. *Nat. Cell Biol.* **5**, 53-58. doi:10.1038/ncb897

Blankenship, J. T., Fuller, M. T. and Zallen, J. A. (2007). The Drosophila homolog of the Exo84 exocyst subunit promotes apical epithelial identity. *J. Cell Sci.* **120**, 3099-3110.

Bonello, T. T. and Peifer, M. (2019). Scribble: A master scaffold in polarity, adhesion, synaptogenesis, and proliferation. *J. Cell Biol.* **218**, 742-756. doi:10.1083/jcb.201810103

Bonello, T. T., Perez-Vale, K. Z., Sumigray, K. D. and Peifer, M. (2018). Rap1 acts via multiple mechanisms to position Canoe and adherens junctions and mediate apical-basal polarity establishment. *Development* **145**, dev157941. doi:10.1242/dev.157941

Bossinger, O., Klebes, A., Segbert, C., Theres, C. and Knust, E. (2001). Zonula adherens formation in Caenorhabditis elegans requires dlg-1, the homologue of the Drosophila gene discs large. *Dev. Biol.* **230**, 29-42. doi:10.1006/dbio.2000.0113

Campanale, J. P., Sun, T. Y. and Montell, D. J. (2017). Development and dynamics of cell polarity at a glance. *J. Cell Sci.* **130**, 1201-1207. doi:10.1242/jcs.188599

Caria, S., Magtoto, C. M., Samiei, T., Portela, M., Lim, K. Y. B., How, J. Y., Stewart, B. Z., Humbert, P. O., Richardson, H. E. and Kvansakul, M. (2018). Drosophila melanogaster Guk-holder interacts with the Scribbled PDZ1 domain and regulates epithelial development with Scribbled and Discs Large. *J. Biol. Chem.* **293**, 4519-4531. doi:10.1074/jbc.M117.817528

Chen, Y. T., Stewart, D. B. and Nelson, W. J. (1999). Coupling assembly of the E-cadherin/beta-catenin complex to efficient endoplasmic reticulum exit and basal-lateral membrane targeting of E- cadherin in polarized MDCK cells. *J. Cell Biol.* **144**, 687-699. doi:10.1083/jcb.144.4.687

Choi, W., Harris, N. J., Sumigray, K. D. and Peifer, M. (2013). Rap1 and Canoe/afadin are essential for establishment of apical-basal polarity in the Drosophila embryo. *Mol. Biol. Cell* **24**, 945-963. doi:10.1091/mbc.e12-10-0736

Choi, W., Acharya, B. R., Peyret, G., Fardin, M. A., Mège, R. M., Ladoux, B., Yap, A. S., Fanning, A. S. and Peifer, M. (2016). Remodeling the zonula adherens in response to tension and the role of afadin in this response. *J. Cell Biol.* **213**, 243-260. doi:10.1083/jcb.201506115

Choi, J., Troyanovsky, R. B., Indra, I., Mitchell, B. J. and Troyanovsky, S. M. (2019). Scribble, Erbin, and Lano redundantly regulate epithelial polarity and apical adhesion complex. *J. Cell Biol.* **218**, 2277-2293. doi:10.1083/jcb.201804201

Chougule, A. B., Hastert, M. C. and Thomas, J. H. (2016). Drak is required for actomyosin organization during Drosophila cellularization. *G3 (Bethesda)* **6**, 819-828. doi:10.1534/g3.115.026401

Cox, R. T., Kirkpatrick, C. and Peifer, M. (1996). Armadillo is required for adherens junction assembly, cell polarity, and morphogenesis during *Drosophila* embryogenesis. *J. Cell Biol.* **134**, 133-148. doi:10.1083/jcb.134.1.133

Fabrowski, P., Necakov, A. S., Mumbauer, S., Loeser, E., Reversi, A., Streichan, S., Briggs, J. A. and De Renzis, S. (2013). Tubular endocytosis drives remodelling of the apical surface during epithelial morphogenesis in Drosophila. *Nat. Commun.* **4**, 2244.

Fehon, R. G., Dawson, I. A. and Artavanis-Tsakonas, S. (1994). A *Drosophila* homologue of membrane-skeleton protein 4.1 is associated with septate junctions and is encoded by the *coracle* gene. *Development* **120**, 545-557.

Firestein, B. L. and Rongo, C. (2001). DLG-1 is a MAGUK similar to SAP97 and is required for adherens junction formation. *Mol. Biol. Cell* **12**, 3465-3475. doi:10.1091/mbc.12.11.3465

Franz, A. and Riechmann, V. (2010). Stepwise polarisation of the Drosophila follicular epithelium. *Dev. Biol.* **338**, 136-147. doi:10.1016/j.ydbio.2009.11.027.

Gateff, E. and Schneiderman, H. A. (1974). Developmental capacities of benign and malignant neoplasms of *Drosophila*. *Roux's Arch. Dev. Biol.* **176**, 23-65. doi:10.1007/BF00577830

Grevengoed, E. E., Fox, D. T., Gates, J. and Peifer, M. (2003). Balancing different types of actin polymerization at distinct sites: roles for Abelson kinase and Enabled. *J. Cell Biol.* **163**, 1267-1279. doi:10.1083/jcb.200307026

Harris, T. J. C. (2012). Adherens junction assembly and function in the Drosophila embryo. *Int. Rev. Cell Mol. Biol.* **293**, 45-83. doi:10.1016/B978-0-12-394304-0.00007-5

Harris, T. J. C. and Peifer, M. (2004). Adherens junction-dependent and -independent steps in the establishment of epithelial cell polarity in Drosophila. *J. Cell Biol.* **167**, 135-147. doi:10.1083/jcb.200406024

Harris, T. J. C. and Peifer, M. (2005). The positioning and segregation of apical cues during epithelial polarity establishment in Drosophila. *J. Cell Biol.* **170**, 813-823. doi:10.1083/jcb.200505127

Harris, T. J. C. and Peifer, M. (2007). aPKC controls microtubule organization to balance adherens junction symmetry and planar polarity during development. *Dev. Cell* **12**, 727-738. doi:10.1016/j.devcel.2007.02.011

Hendrick, J., Franz-Wachtel, M., Moeller, Y., Schmid, S., Macek, B. and Olayioye, M. A. (2016). The polarity protein Scribble positions DLC3 at adherens junctions to regulate Rho signaling. *J. Cell Sci.* **129**, 3583-3596. doi:10.1242/jcs.190074

Homem, C. C. and Peifer, M. (2008). Diaphanous regulates myosin and adherens junctions to control cell contractility and protrusive behavior during morphogenesis. *Development* **135**, 1005-1018. doi:10.1242/dev.016337

Hong, Y. (2018). aPKC: the kinase that phosphorylates cell polarity. *F1000Res* **7**, F1000. doi:10.12688/f1000research.14427.1

Hunter, C. and Wieschaus, E. (2000). Regulated expression of nullo is required for the formation of distinct apical and basal adherens junctions in the Drosophila blastoderm. *J. Cell Biol.* **150**, 391-401. doi:10.1083/jcb.150.2.391

Hutterer, A., Betschinger, J., Petronczki, M. and Knoblich, J. A. (2004). Sequential roles of Cdc42, Par-6, aPKC, and Lgl in the establishment of epithelial polarity during Drosophila embryogenesis. *Dev. Cell* **6**, 845-854. doi:10.1016/j.devcel.2004.05.003

Ivarsson, Y., Arnold, R., McLaughlin, M., Nim, S., Joshi, R., Ray, D., Liu, B., Teyra, J., Pawson, T., Moffat, J. et al. (2014). Large-scale interaction profiling of PDZ domains through proteomic peptide-phage display using human and viral phage peptidomes. *Proc. Natl. Acad. Sci. USA* **111**, 2542-2547. doi:10.1073/pnas.1312296111

Köppen, M., Simske, J. S., Sims, P. A., Firestein, B. L., Hall, D. H., Radice, A. D., Rongo, C. and Hardin, J. D. (2001). Cooperative regulation of AJM-1 controls junctional integrity in Caenorhabditis elegans epithelia. *Nat. Cell Biol.* **3**, 983-991. doi:10.1038/ncb1101-983

Kullmann, L. and Krahn, M. P. (2018). Redundant regulation of localization and protein stability of DmPar3. *Cell. Mol. Life Sci.* **75**, 3269-3282. doi:10.1007/s00018-018-2792-1

Laprise, P., Beronja, S., Silva-Gagliardi, N. F., Pellikka, M., Jensen, A. M., McGlade, C. J. and Tepass, U. (2006). The FERM protein Yurt is a negative regulatory component of the Crumbs complex that controls epithelial polarity and apical membrane size. *Dev. Cell* **11**, 363-374. doi:10.1016/j.devcel.2006.06.001

Laprise, P., Lau, K. M., Harris, K. P., Silva-Gagliardi, N. F., Paul, S. M., Beronja, S., Beitel, G. J., McGlade, C. J. and Tepass, U. (2009). Yurt, Coracle, Neurexin IV and the Na(+),K(+)-ATPase form a novel group of epithelial polarity proteins. *Nature* **459**, 1141-1145. doi:10.1038/nature08067

Lee, O. K., Frese, K. K., James, J. S., Chadda, D., Chen, Z. H., Javier, R. T. and Cho, K. O. (2003). Discs-Large and Strabismus are functionally linked to plasma membrane formation. *Nat. Cell Biol.* **5**, 987-993.

Legouis, R., Gansmuller, A., Sookhareea, S., Bosher, J. M., Baillie, D. L. and Labouesse, M. (2000). LET-413 is a basolateral protein required for the assembly of adherens junctions in Caenorhabditis elegans. *Nat. Cell Biol.* **2**, 415-422. doi:10.1038/35017046

Lockwood, C. A., Lynch, A. M. and Hardin, J. (2008). Dynamic analysis identifies novel roles for DLG-1 subdomains in AJM-1 recruitment and LET-413-dependent apical focusing. *J. Cell Sci.* **121**, 1477-1487. doi:10.1242/jcs.017137

Lohia, M., Qin, Y. and Macara, I. G. (2012). The Scribble polarity protein stabilizes E-cadherin/p120-catenin binding and blocks retrieval of E-cadherin to the Golgi. *PLoS ONE* **7**, e51130. doi:10.1371/journal.pone.0051130

Mathew, D., Gramates, L. S., Packard, M., Thomas, U., Bilder, D., Perrimon, N., Gorczyca, M. and Budnik, V. (2002). Recruitment of scribble to the synaptic scaffolding complex requires GUK-holder, a novel DLG binding protein. *Curr. Biol.* **12**, 531-539. doi:10.1016/S0960-9822(02)00758-3

Mavrakis, M., Rikhy, R. and Lippincott-Schwartz, J. (2009). Plasma membrane polarity and compartmentalization are established before cellularization in the fly embryo. *Dev. Cell* **16**, 93-104. doi:10.1016/j.devcel.2008.11.003

McDonald, J. A., Khodyakova, A., Aranjuez, G., Dudley, C. and Montell, D. J. (2008). PAR-1 kinase regulates epithelial detachment and directional protrusion of migrating border cells. *Curr. Biol.* **18**, 1659-1667. doi:10.1016/j.cub.2008.09.041

McGill, M. A., McKinley, R. F. and Harris, T. J. (2009). Independent cadherin-catenin and Bazooka clusters interact to assemble adherens junctions. *J. Cell Biol.* **185**, 787-796. doi:10.1083/jcb.200812146

McKinley, R. F. and Harris, T. J. (2012). Displacement of basolateral Bazooka/PAR-3 by regulated transport and dispersion during epithelial polarization in Drosophila. *Mol. Biol. Cell* **23**, 4465-4471. doi:10.1091/mbc.e12-09-0655

McKinley, R. F., Yu, C. G. and Harris, T. J. (2012). Assembly of Bazooka polarity landmarks through a multifaceted membrane-association mechanism. *J. Cell Sci.* **125**, 1177-1190. doi:10.1242/jcs.091884

McMahon, L., Legouis, R., Vonesch, J. L. and Labouesse, M. (2001). Assembly of C. elegans apical junctions involves positioning and compaction by LET-413 and protein aggregation by the MAGUK protein DLG-1. *J. Cell Sci.* **114**, 2265-2277.

Métais, J.-Y., Navarro, C., Santoni, M.-J., Audebert, S. and Borg, J.-P. (2005). hScrib interacts with ZO-2 at the cell-cell junctions of epithelial cells. *FEBS Lett.* **579**, 3725-3730. doi:10.1016/j.febslet.2005.05.062

Müller, H.-A. J. and Wieschaus, E. (1996). *armadillo*, *bazooka*, and *stardust* are critical for formation of the zonula adherens and maintenance of the polarized blastoderm epithelium in *Drosophila*. *J. Cell Biol.* **134**, 149-165. doi:10.1083/jcb.134.1.149

Murdoch, J. N., Henderson, D. J., Doudney, K., Gaston-Massuet, C., Phillips, H. M., Paternotte, C., Arkell, R., Stanier, P. and Copp, A. J. (2003). Disruption of scribble (Scrb1) causes severe neural tube defects in the circletail mouse. *Hum. Mol. Genet.* **12**, 87-98. doi:10.1093/hmg/ddg014

Navarro, C., Nola, S., Audebert, S., Santoni, M.-J., Arsanto, J.-P., Ginestier, C., Marchetto, S., Jacquemier, J., Isnardon, D., Le Bivic, A. et al. (2005).

Junctional recruitment of mammalian Scribble relies on E-cadherin engagement. *Oncogene* **24**, 4330-4339. doi:10.1038/sj.onc.1208632

Ni, J. Q., Zhou, R., Czech, B., Liu, L. P., Holderbaum, L., Yang-Zhou, D., Shim, H. S., Tao, R., Handler, D., Karpowicz, P. et al. (2011). A genome-scale shRNA resource for transgenic RNAi in Drosophila. *Nat. Methods* **8**, 405-407. doi:10.1038/nmeth.1592

Oshima, K. and Fehon, R. G. (2011). Analysis of protein dynamics within the septate junction reveals a highly stable core protein complex that does not include the basolateral polarity protein Discs large. *J. Cell Sci.* **124**, 2861-2871. doi:10.1242/jcs.087700

Pearson, H. B., Perez-Mancera, P. A., Dow, L. E., Ryan, A., Tennstedt, P., Bogani, D., Elsum, I., Greenfield, A., Tuveson, D. A., Simon, R. et al. (2011). SCRIB expression is deregulated in human prostate cancer, and its deficiency in mice promotes prostate neoplasia. *J. Clin. Invest.* **121**, 4257-4267. doi:10.1172/JCI58509

Pelissier, A., Chauvin, J. P. and Lecuit, T. (2003). Trafficking through Rab11 endosomes is required for cellularization during Drosophila embryogenesis. *Curr. Biol.* **13**, 1848-1857.

Qin, Y., Capaldo, C., Gumbiner, B. M. and Macara, I. G. (2005). The mammalian Scribble polarity protein regulates epithelial cell adhesion and migration through E-cadherin. *J. Cell Biol.* **171**, 1061-1071. doi:10.1083/jcb.200506094

Roeth, J. F., Sawyer, J. K., Wilner, D. A. and Peifer, M. (2009). Rab11 helps maintain apical crumbs and adherens junctions in the Drosophila embryonic ectoderm. *PLoS ONE* **4**, e7634. doi:10.1371/journal.pone.0007634

Roux, K. J., Kim, D. I., Raida, M. and Burke, B. (2012). A promiscuous biotin ligase fusion protein identifies proximal and interacting proteins in mammalian cells. *J. Cell Biol.* **196**, 801-810. doi:10.1083/jcb.201112098

Sarpal, R., Pellikka, M., Patel, R. R., Hui, F. Y. W., Godt, D. and Tepass, U. (2012). Mutational analysis supports a core role for Drosophila alpha-catenin in adherens junction function. *J. Cell Sci.* **125**, 233-245. doi:10.1242/jcs.096644

Sawyer, J. K., Harris, N. J., Slep, K. C., Gaul, U. and Peifer, M. (2009). The Drosophila afadin homologue Canoe regulates linkage of the actin cytoskeleton to adherens junctions during apical constriction. *J. Cell Biol.* **186**, 57-73. doi:10.1083/jcb.200904001

Schmidt, A. and Grosshans, J. (2018). Dynamics of cortical domains in early Drosophila development. *J. Cell Sci.* **131**, jcs212795. doi:10.1242/jcs.212795

Sears, R. M., May, D. G. and Roux, K. J. (2019). BioID as a tool for protein-proximity labeling in living cells. *Methods Mol. Biol.* **2012**, 299-313. doi:10.1007/978-1-4939-9546-2_15

Sokac, A. M. and Wieschaus, E. (2008). Zygotically controlled F-actin establishes cortical compartments to stabilize furrows during Drosophila cellularization. *J. Cell Sci.* **121**, 1815-1824.

Staller, M. V., Yan, D., Randklev, S., Bragdon, M. D., Wunderlich, Z. B., Tao, R., Perkins, L. A., Depace, A. H. and Perrimon, N. (2013). Depleting gene activities in early Drosophila embryos with the “maternal-Gal4-shRNA” system. *Genetics* **193**, 51-61. doi:10.1534/genetics.112.144915

Stephens, R., Lim, K., Portela, M., Kvansakul, M., Humbert, P. O. and Richardson, H. E. (2018). The scribble cell polarity module in the regulation of cell signaling in tissue development and tumorigenesis. *J. Mol. Biol.* **430**, 3585-3612. doi:10.1016/j.jmb.2018.01.011

Tanaka, T. and Nakamura, A. (2008). The endocytic pathway acts downstream of Oskar in Drosophila germ plasm assembly. *Development* **135**, 1107-1117. doi:10.1242/dev.017293

Tanentzapf, G. and Tepass, U. (2003). Interactions between the crumbs, lethal giant larvae and bazooka pathways in epithelial polarization. *Nat. Cell Biol.* **5**, 46-52. doi:10.1038/ncb896

Tepass, U. (2012). The apical polarity protein network in Drosophila epithelial cells: regulation of polarity, junctions, morphogenesis, cell growth, and survival. *Annu. Rev. Cell Dev. Biol.* **28**, 655-685. doi:10.1146/annurev-cellbio-092910-154033

Tepass, U., Gruszynski-DeFeo, E., Haag, T. A., Omatyar, L., Török, T. and Hartenstein, V. (1996). *Shotgun* encodes *Drosophila* E-cadherin and is preferentially required during cell rearrangement in the neurectoderm and other morphogenetically active epithelia. *Genes Dev.* 10, 672-685. doi:10.1101/gad.10.6.672

Truong Quang, B.-A., Mani, M., Markova, O., Lecuit, T. and Lenne, P.-F. (2013). Principles of E-cadherin supramolecular organization in vivo. *Curr. Biol.* **23**, 2197-2207. doi:10.1016/j.cub.2013.09.015

Van Itallie, C. M., Aponte, A., Tietgens, A. J., Gucek, M., Fredriksson, K. and Anderson, J. M. (2013). The N and C termini of ZO-1 are surrounded by distinct proteins and functional protein networks. *J. Biol. Chem.* **288**, 13775-13788. doi:10.1074/jbc.M113.466193

Wang, Y.-C., Khan, Z., Kaschube, M. and Wieschaus, E. F. (2012). Differential positioning of adherens junctions is associated with initiation of epithelial folding. *Nature* **484**, 390-393. doi:10.1038/nature10938

Wieschaus, E. and Nüsslein-Volhard, C. (1986). Looking at embryos. In *Drosophila, A Practical Approach* (ed. D. B. Roberts), pp. 199-228. Oxford, England: IRL Press.

Woods, D. F. and Bryant, P. J. (1991). The *discs-large* tumor suppressor gene of *Drosophila* encodes a guanylate kinase homolog localized at septate junctions. *Cell* **66**, 451-464. doi:10.1016/0092-8674(81)90009-X

Woods, D. F., Hough, C., Peel, D., Callaini, G. and Bryant, P. J. (1996). Dlg protein is required for junction structure, cell polarity, and proliferation control in *Drosophila* epithelia. *J. Cell Biol.* **134**, 1469-1482. doi:10.1083/jcb.134.6.1469

Yates, L. L., Schnatwinkel, C., Hazelwood, L., Chessum, L., Paudyal, A., Hilton, H., Romero, M. R., Wilde, J., Bogani, D., Sanderson, J. et al. (2013). Scribble is required for normal epithelial cell-cell contacts and lumen morphogenesis in the mammalian lung. *Dev. Biol.* **373**, 267-280. doi:10.1016/j.ydbio.2012.11.012

Zarbalis, K., May, S. R., Shen, Y., Ekker, M., Rubenstein, J. L. and Peterson, A. S. (2004). A focused and efficient genetic screening strategy in the mouse: identification of mutations that disrupt cortical development. *PLoS Biol.* **2**, E219. doi:10.1371/journal.pbio.0020219

Zeitler, J., Hsu, C. P., Dionne, H. and Bilder, D. (2004). Domains controlling cell polarity and proliferation in the Drosophila tumor suppressor Scribble. *J. Cell Biol.* **167**, 1137-1146. doi:10.1083/jcb.200407158

Zhang, Y., Yeh, S., Appleton, B. A., Held, H. A., Kausalya, P. J., Phua, D. C., Wong, W. L., Lasky, L. A., Wiesmann, C., Hunziker, W. et al. (2006). Convergent and divergent ligand specificity among PDZ domains of the LAP and zonula occludens (ZO) families. *J. Biol. Chem.* **281**, 22299-22311. doi:10.1074/jbc.M602902200

Zhang, J., Schulze, K. L., Hiesinger, P. R., Suyama, K., Wang, S., Fish, M., Acar, M., Hoskins, R. A., Bellen, H. J. and Scott, M. P. (2007). Thirty-one flavors of Drosophila rab proteins. *Genetics* **176**, 1307-1322. doi:10.1534/genetics.106.066761

A Intensity of Scrib, Dlg, Arm and Cno in the AJ vs. basolateral region measured from MIPs (Figs. 1I, 3H, 4J, and 7Q)

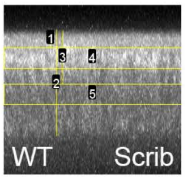

1. 2.5 µm from apical surface (24.5 px)
2. Define total membrane length
3. Define 50% membrane length
4. 'AJ zone' defined by 26 x 3 µm (250 x 29 px) ROI
5. 'Basolateral zone', positioned at 50% membrane length and defined by 26 x 3 µm (250 x 29 px) ROI

B Dlg apical intensity measured from single cross sections (Fig. 2G,N)

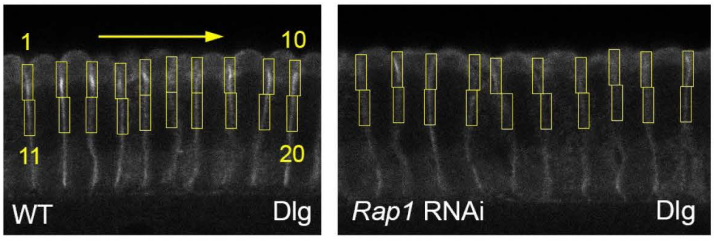

1-10. 10 consecutive apical ROIs (15 x 50 px)
11-20. 10 consecutive basal ROIs (15 x 50 px)

C Intensity of Baz in the apical vs. basolateral region measured from MIPs (Fig. 5G)

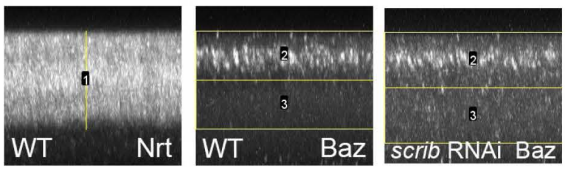

1. Total membrane length determined by co-stain with Neurotactin
2. Total apical region taken as upper 50% of membrane
3. Total basal region taken as lower 50% of membrane

D Par-1 cortical signal measured from the basolateral region of orthogonal reconstructions (Fig. 7E,F)

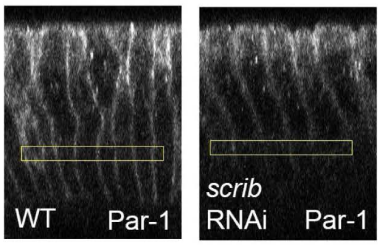

200 x 20 px ROI was placed across the basolateral membrane (positioned below nucleus) intersecting 6-7 cortical points per embryo.

E Spread of the apical AJ zone as a fraction of total cell length measured from MIPs (Fig. 8R)

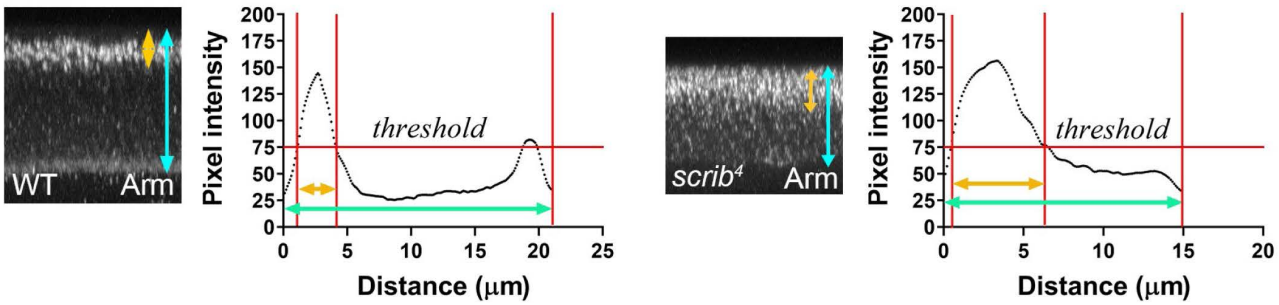

Figure S1. Illustration of approaches used for quantification. A-E. All measurements were taken from cellularizing (stage 5) or early stage 6 embryos. For A,C, and E Maximum Intensity Projections (MIP) were generated by acquiring z-stacks through the embryo with a 0.3 µm step size and digital zoom of 2. ZEN 2009 software was used to crop stacks to 250 × 250 pixels along the xy-axis and to project xyz-stacks along the y-axis. In B intensities were measured from single cross sections, while in D intensities were measured from single plane orthogonal reconstructions. A. In Fig. 1I, 3H, 4J and 7Q, intensity of Scrib, Dlg, Arm or Cno in the subapical region (AJ zone, box 4) was reported as a ratio over signal intensity in the basolateral region (box 5) measured from MIPs. The apical space above the spot AJ (line 1) was defined as 2.5 µm for embryos with a total membrane length of >15 µm or 1.5 µm for embryos with a total membrane length of 8-15 µm. B. In Fig. 2G,N, apical enrichment of Dlg was reported as a ratio between total signal intensity in a defined apical ROI, over total signal intensity from a more basal region. Total apical intensity was measured by selecting 10 consecutive ROIs, positioned over the cortical membrane, with the upper bound of the box aligned with the apical surface (ROI 1-10). A second set of identically sized boxes (ROI 11-20) were positioned immediately below ROI 1-10, with exact placement adjusted to centre the box over the cortical membrane. C. In Fig. 5G, apical enrichment of Baz was reported as a ratio of total pixel intensity in the top 50% over the lower 50% of the membrane, measured from MIPs. D. To measure Par-1 cortical localization along the basolateral membrane (reported in Fig. 7E,F), ZEN software was used to select a 250 x 250 pixel ROI in the xy dimension through a series of z slices which were then projected orthogonally. In ImageJ, a 200 x 20 pixel box was drawn along the basolateral domain spanning approximately 6-7 individual cells (thus placing the box below the nucleus) and average pixel intensity along the selected region was determined using the Plot Profile function. Numerical values generated in ImageJ were graphed in GraphPad Prism. E. To determine the expansion of the junctional zone in *scrib*^{4} mutants (Fig. 8R), MIPs were rotated 90° counterclockwise and analyzed using the Plot Profile function in ImageJ to generate values of average pixel intensity along the apical-basal axis (defined on graphs as distance in µm). Images were thresholded so that the region of the pixel plot defined by an average pixel intensity of 75 or greater was recorded and reported as a ratio of total membrane length.

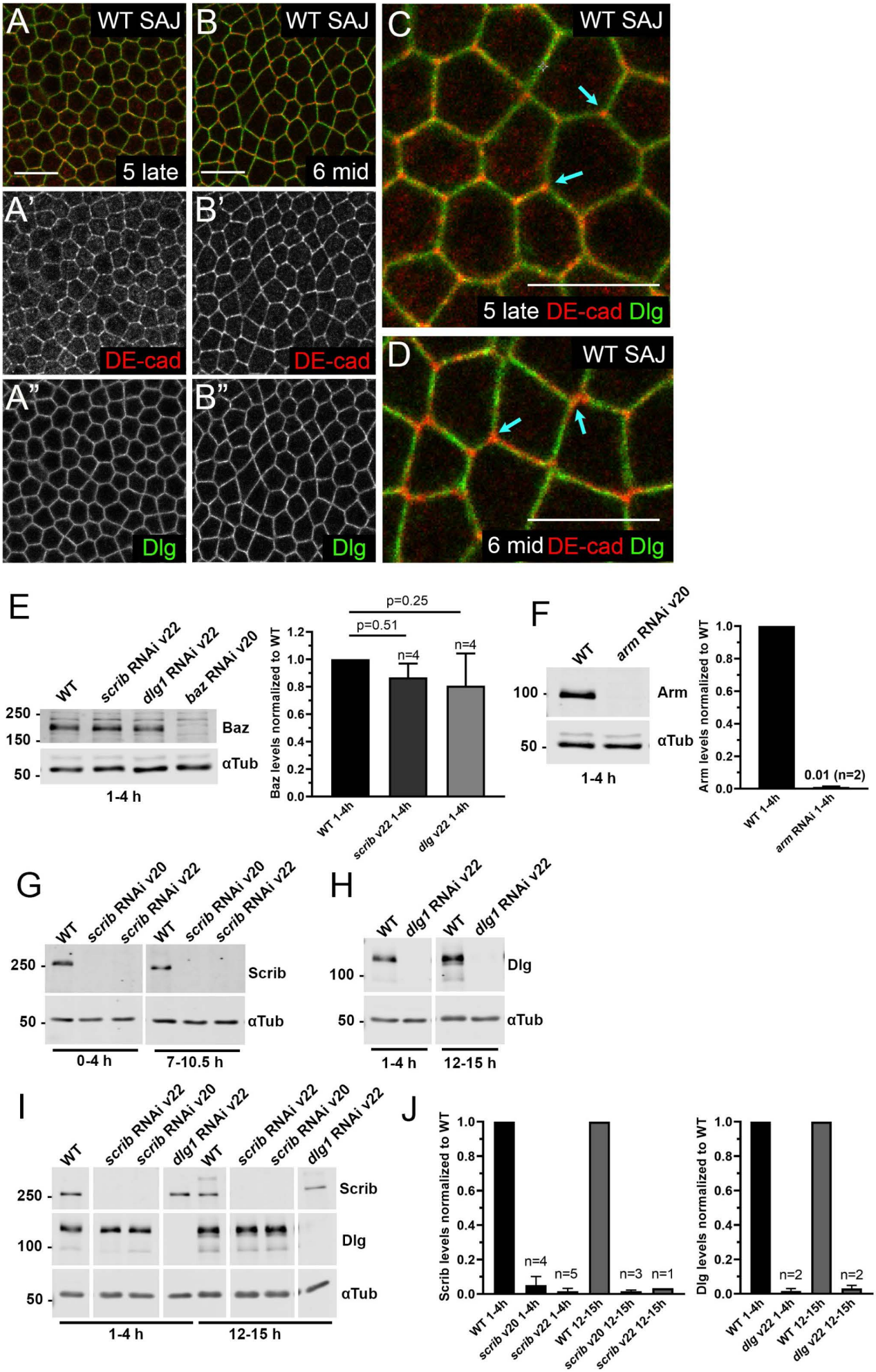
A
WT SAJ
5 late
B
WT SAJ
6 mid
C
WT SAJ
5 late DE-cad Dlg
A'
DE-cad
B'
DE-cad
A''
Dlg
B''
Dlg
D
WT SAJ
6 mid DE-cad Dlg
E
WT
scrib RNAi v22
dlg1 RNAi v22
baz RNAi v20
250
150
50
Baz
αTub
1-4 h
p=0.25
p=0.51
n=4
n=4
Baz levels normalized to WT
WT 1-4h
scrib v22 1-4h
dlg v22 1-4h
F
WT
arm RNAi v20
100
50
Arm
αTub
1-4 h
Arm levels normalized to WT
0.01 (n=2)
WT 1-4h
arm RNAi 1-4h
G
WT
scrib RNAi v20
scrib RNAi v22
WT
scrib RNAi v20
scrib RNAi v22
250
50
Scrib
αTub
0-4 h
7-10.5 h
H
WT
dlg1 RNAi v22
WT
dlg1 RNAi v22
100
50
Dlg
αTub
1-4 h
12-15 h
I
WT
scrib RNAi v22
scrib RNAi v20
dlg1 RNAi v22
WT
scrib RNAi v22
scrib RNAi v20
dlg1 RNAi v22
250
100
50
Scrib
Dlg
αTub
1-4 h
12-15 h
J
Scrib levels normalized to WT
n=4
n=5
n=3
n=1
WT 1-4h
scrib v20 1-4h
scrib v22 1-4h
WT 12-15h
scrib v20 12-15h
scrib v22 12-15h
Dlg levels normalized to WT
n=2
n=2
WT 1-4h
dlg v22 1-4h
WT 12-15h
dlg v22 12-15h

Figure S2. Dlg enrichment at AJs and assessment of our *scrib* and *dlg-RNAi* tools. A- D. Dlg in cellularizing (stage 5; A,C) and gastrulation onset (stage 6; B,D) embryos, relative to AJ proteins. *En face* sections through SAJs at the level of highest enrichment. Arrows in C,D=tricellular junctions, where DE-cad is enriched but Dlg is not. Scalebars=10µm. E-J. Representative Western blots of embryonic extracts at the indicated ages in wildtype and after expression of our chosen RNAi lines, driven by a pair of strong maternal GAL4 drivers (MatGAL4). E. *scrib-RNAi* and *dlg*-RNAi led to very modest reductions in total Baz levels while our *baz-RNAi* line strongly reduced Baz accumulation. F. Our *arm-RNAi* line strongly reduced Arm accumulation. G. Two independent *scrib-RNAi* lines effectively knockdown maternal and zygotic Scrib during early development and mid-embryogenesis. Most experiments were carried out with the valium 22 line, but key conclusions were verified with the valium 20 line. H. Effective knockdown of maternal and zygotic Dlg by the *dlg-RNAi* line used in this study. I. *scrib-RNAi* did not substantially alter Dlg levels, nor did *dlg-RNAi* alter Scrib levels. J. Quantification of blots in G,H. In E,F, and J quantification = mean±sd. normalized to wildtype.

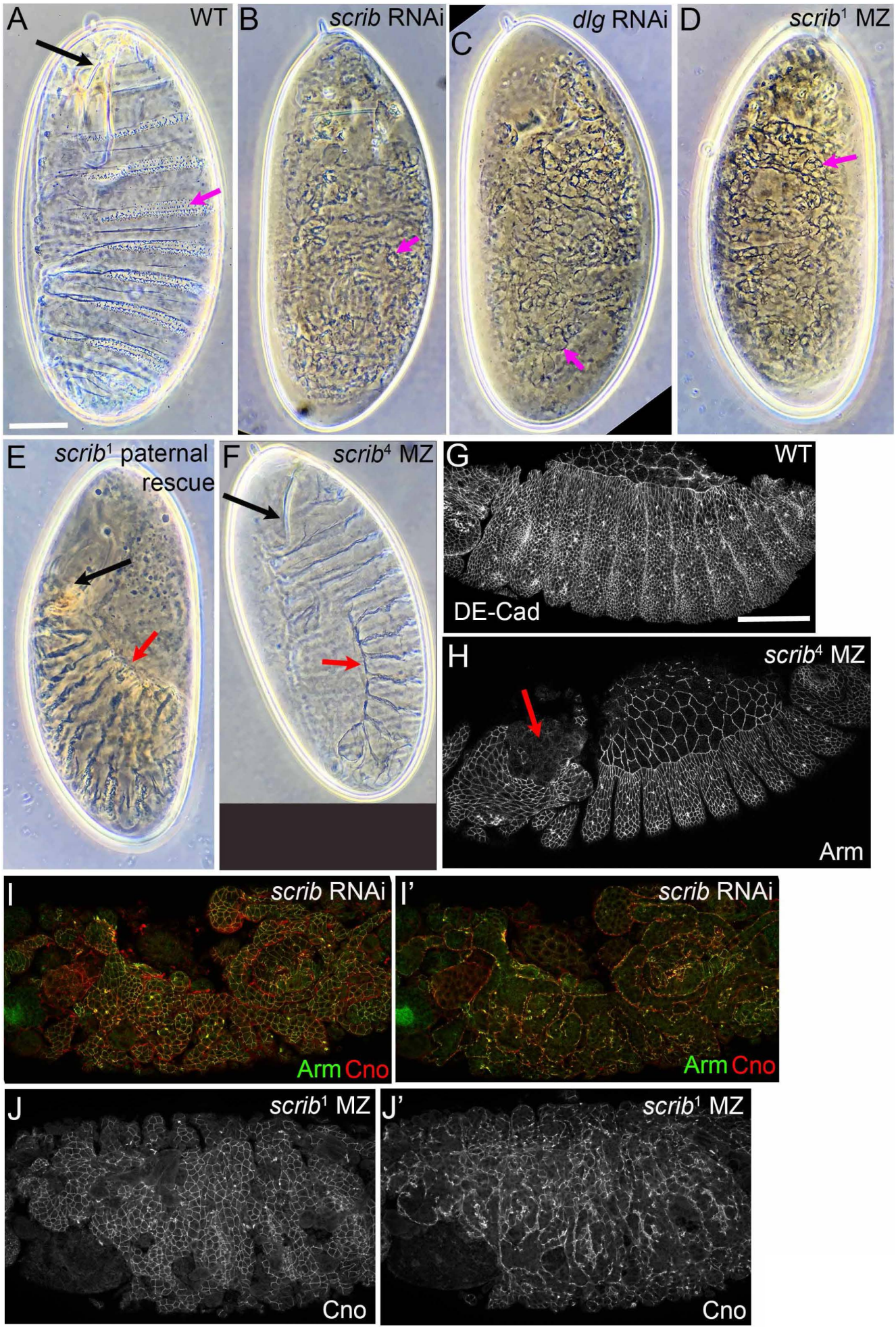

Figure S3. Comparison of cuticle phenotypes between *scrib-RNAi*, *dlg-RNAi* and *scrib* mutants. A-F. Cuticles, anterior up. A. Wildtype. Note intact head skeleton (black arrow) and intact epidermis with alternating denticle belts (magenta arrow) and naked cuticle. B-D. *scrib-RNAi* (B) and *dlg-RNAi* (C) phenocopy the strong *scrib*^{1} allele (D) showing the characteristic "scribbled" cuticle phenotype with remnant vesicles and tubules of cuticle (arrows). E. Paternally rescued *scrib*^{1} mutant—morphogenesis, including head involution (black arrow) and dorsal closure (red arrow) fail, but epidermal cuticle integrity is largely restored. F. Maternal/zygotic *scrib*^{4} mutant. Head involution (black arrow) and dorsal closure (red arrow) fail. G-J. Wildtype vs. *scrib*^{4} maternal/zygotic mutant, *scrib-RNAi* embryo and *scrib*^{1} maternal/zygotic mutant during dorsal closure. In the *scrib*^{4} mutant (H) the epidermis is intact but head involution has failed (arrow). In contrast, at this stage after *scrib-RNAi* (I) or in a *scrib*^{1} maternal/zygotic, mutant (J), while some junctional polarity has been re-established (as illustrated by apical Arm and/or Cno staining), cross sectional images reveal that the epidermis is fragmented into cortical balls or folds. Scale bars=50μm.

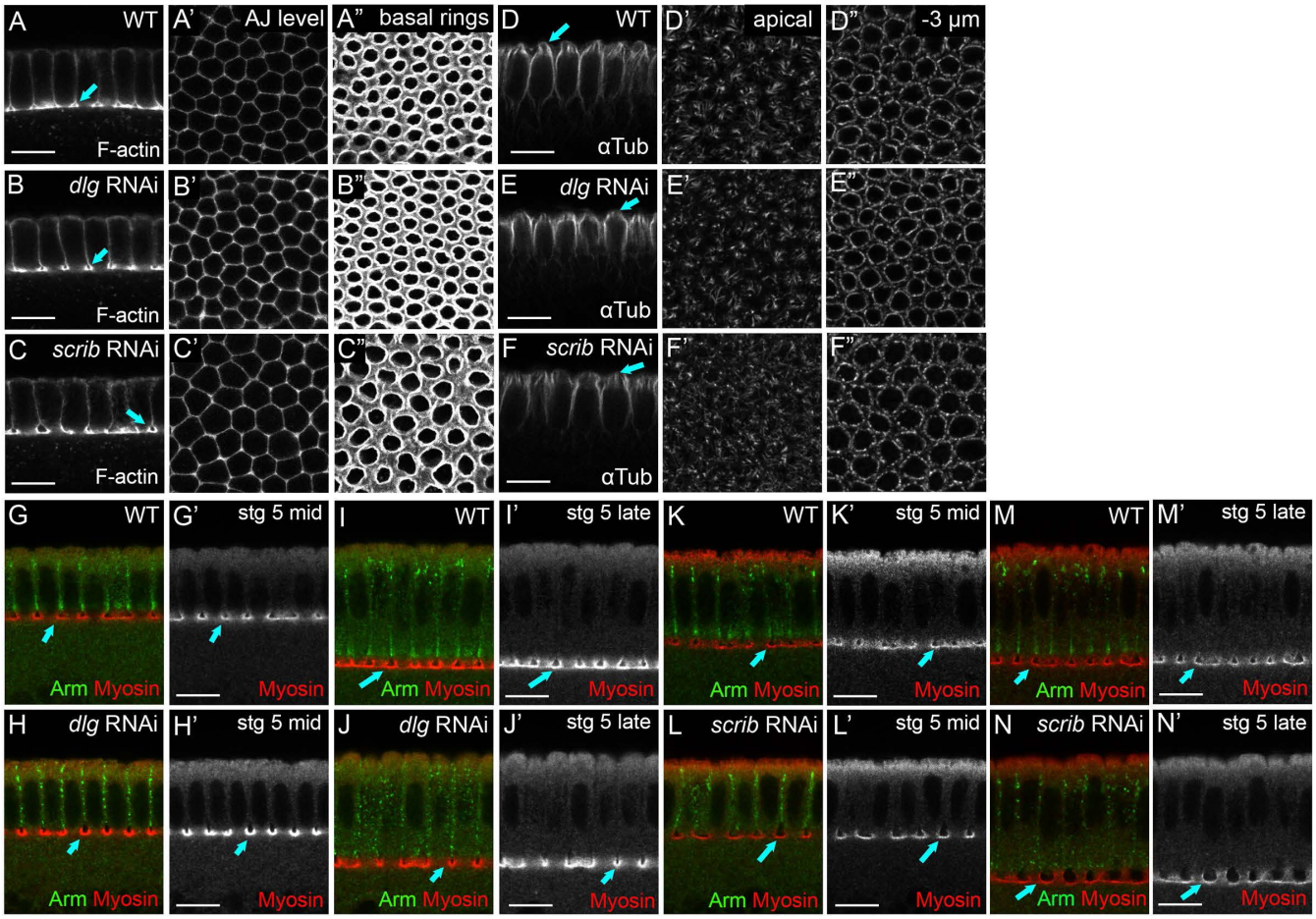

Figure S4. Neither Scrib nor Dlg knockdown alters basic cytoskeletal polarity at cellularization. Embryos, mid- to late cellularization, genotypes and antigens indicated. A. In wildtype, actin is found all along the cortex, including at the level of the nascent AJs (A') but is substantially enriched at the cellularization front and the closing basal rings (A arrow, A"). B,C. This is unaltered after *dlg* or *scrib-RNAi*. D. In wildtype tubulin forms inverted baskets (D,D") nucleated from centrosomes above each nucleus (D arrow, D',D"). E,F. This is unaltered after *dlg* or *scrib-RNAi*. G,I,K,M. Myosin localizes to the cellularization front (arrows) and more diffusely to an apical pool. H,J,L,N. Once again, these features are unaltered after *dlg* or *scrib-RNAi*. Scale bars=20µm.

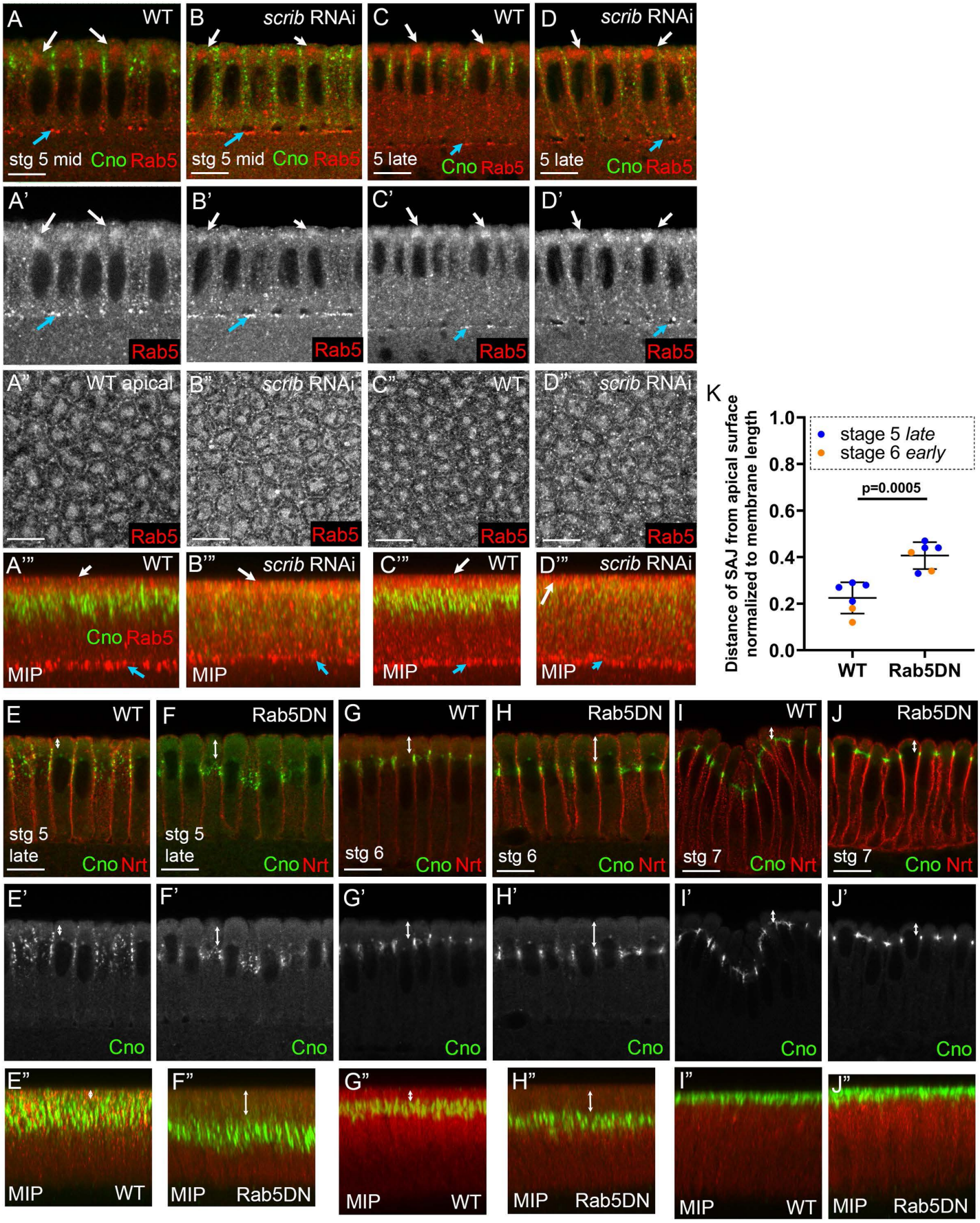

Figure S5. Rab5 localizes to an apical vesicular structure near nascent AJs and regulates precise apical positioning of SAJs. Cross-sections (A-D,E-J), MIPs (A'"-D'",E"-J"), or apical *en face* sections (A"-D"). A-D. During cellularization of both wildtype and *scrib-RNAi* embryos, Rab5 localizes to the furrow front (cyan arrows) and to an apical vesicular compartment (A-D, A"-D",A'"-D'",white arrows). E-J. Rab5DN does not block Cno assembly into SAJs but does lead to a basal shift in SAJ positioning during cellularization (E vs F, white arrows) and early gastrulation (G vs H, white arrows). I,J. Junctional positioning is restored by stage 7 (I vs J,white arrows). K. Quantification of junctional positioning. Each dot on the graph represents a measurement taken from an individual embryo (mean±sd.). Scale bars=10μm.

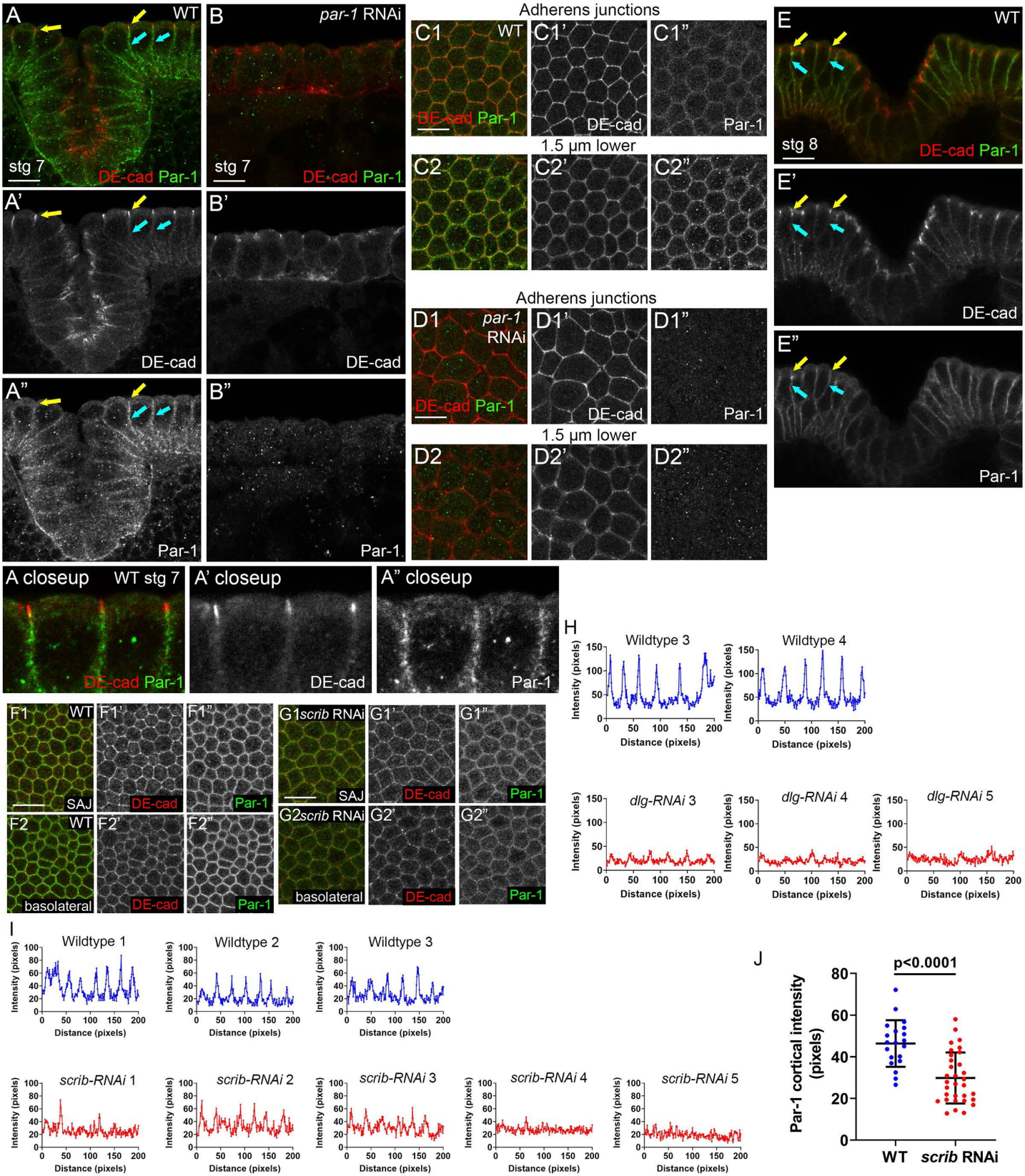

Figure S6. Par-1 and AJs largely segregate by stage 8 and *scrib-RNAi* reduces cortical accumulation of Par-1. A-G. Embryos, stage, genotype and antigens indicated. A,C. In wildtype, by stage 7 AJs move apically and localize largely apical to Par-1 (A yellow arrows, A closeup, C1), while Par-1 remains on the basolateral cortex (A cyan arrows, C2). B,D. Validation of *par-1-RNAi* reagent. *par-1-RNAi* essentially eliminated Par-1 signal, as detected by immunofluorescence. E. At stage 8 AJs continue to localize apical to Par-1. F-G. After *scrib-RNAi* (G) cortical Par-1 is reduced both at the level of the SAJs (F1" vs. G1") and more basolaterally (F2" vs G2"). Scale bars=10μm. H-I. Signal intensity at the basolateral membrane across the cell in cross-sections. In wildtype clear periodic peaks were observed at the cortex, which were significantly reduced after *dlg-RNAi* (H), or *scrib-RNAi* (I). (J) Quantification of maximum peak height over baseline in wildtype versus *scrib-RNAi* (mean±sd.).

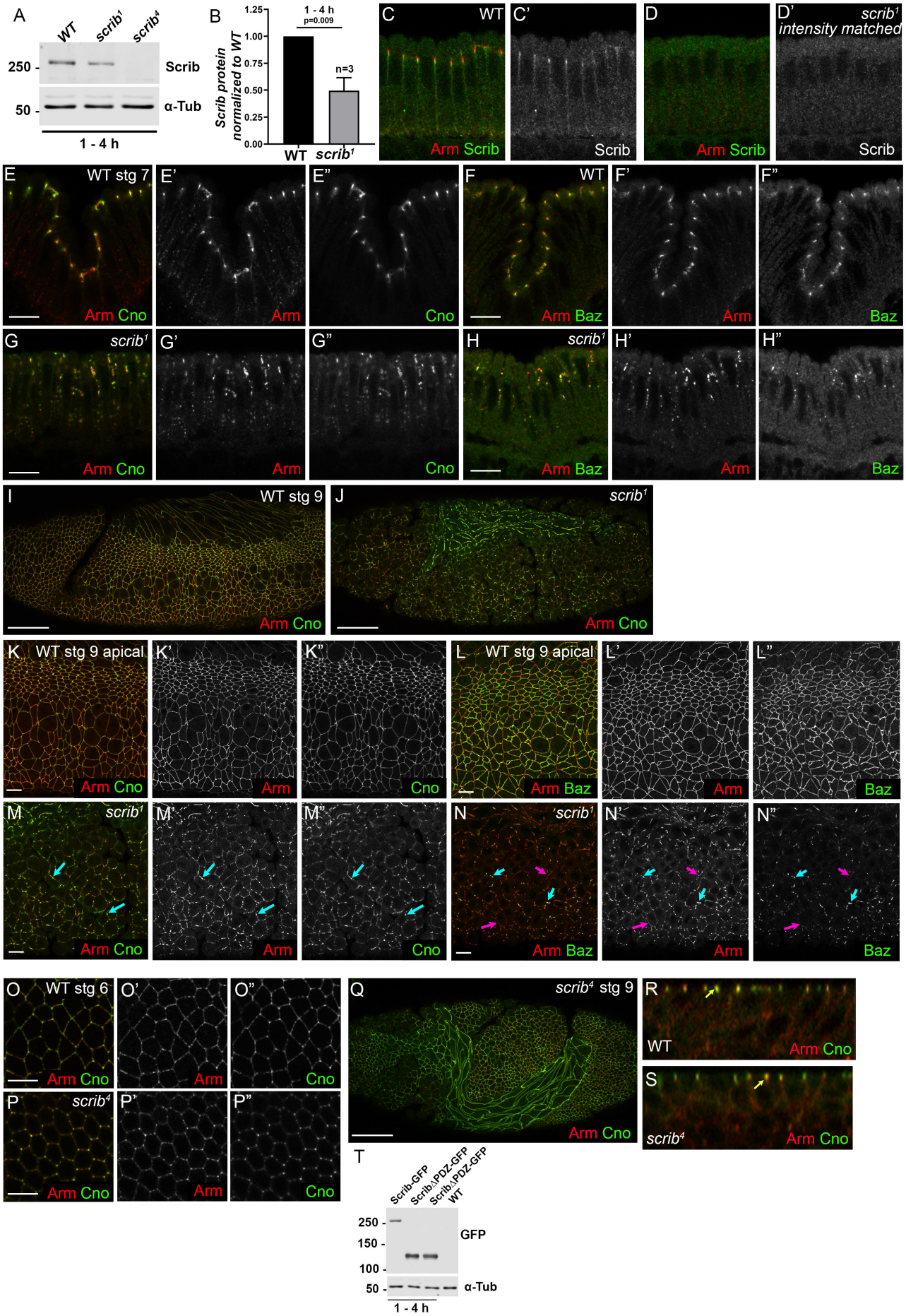

Figure S7. *scrib[1]* encodes a stable protein that does not localize to the cortex and *scrib[1]* mutants phenocopy *scrib*-RNAi after gastrulation onset. A,B. Immunoblot of wildtype versus maternal + maternal/zygotic *scrib[1]* and *scrib[4]* mutants and quantification. The protein encoded by *scrib[1]* accumulates at about 50% the level of wildtype Scrib (mean±sd. normalized to wildtype). The protein encoded by *scrib[4]* lacks the antibody epitope and serves as a control. C-N. Wildtype vs. *scrib[1]* maternal/zygotic mutant embryos C,D. Cellularization. Intensity matched images. The protein encoded by *scrib[1]* is not enriched at the cortex. E-H. Gastrulation onset. Tight apical focusing of Arm, Cno and Baz into belt junctions (E,F) fails in *scrib[1]* mutants, with junctional puncta distributed along the basolateral cortex (G,H). I-N. Stage 9. In wildtype, Arm, Cno and Baz localize continuously in belt AJs (I,K,L). In contrast, in *scrib[1]* mutants AJs fragment and cells begin to separate. Arm and Cno largely co-localize in junctional fragments (M,arrows), but Baz is more rapidly lost than Arm (N,magenta vs cyan arrows). O-S. Wildtype vs. *scrib[4]* at gastrulation onset (stage 6). *scrib[4]* mutants are delayed in the SAJ to belt AJ transition, exhibiting enhanced tricellular junction enrichment (O vs P). S-U. By stage 9 *scrib[4]* mutants cell shapes remain abnormal (Q) but junctional proteins repolarize (R,S,yellow arrows). T. The Mat-GAL4 driver was used to express either UAS.ScribFL::GFP and UAS.ScribΔPDZ::GFP (similar in structure to the protein encoded by *scrib4*) and embryo extracts were immunoblotted with antibodies to GFP or to tubulin as a loading control. In lane 2 UAS.ScribΔPDZ::GFP was coexpressed with our *scrib*-RNAi construct which does not target the truncated protein. Scalebars in I,J,Q=50μm, K-N=20μm. All others=10μm.

Table S1. Fly stocks, antibodies and probes

Fly Stock		Source
UAS.*scrib* RNAi (valium20; BL35748)		Bloomington *Drosophila* Stock Center (BDSC)
UAS.*scrib* RNAi (valium22; BL38199)		BDSC
UAS.*dlg1* RNAi (valium22; BL35286)		BDSC
UAS.*arm* RNAi (valium20; BL35004)		BDSC
UAS.*Rap1* RNAi (valium20; BL35047)		BDSC
UAS.*baz* RNAi (valium20; BL35002)		BDSC
UAS.*par-1* RNAi (valium20; BL32410)		BDSC
UASp.YFP.Rab5.S43N (BL9771)		BDSC
FRT82B ovoD1-18 (BL2149)		BDSC
hsFLP;;Dr[Mio]/Tm3 (BL7)		BDSC
scrib^{1} FRT82B/Tm3		Kindly provided by David Bilder (Bilder and Perrimon, 2000)
scrib^{4} FRT82B/Tm6C		Kindly provided by David Bilder (Zeitler et al., 2004)
Antibodies/probes	**Dilution (IF, WB*)**	**Source**
Primary antibodies		
Anti-Nrt (mouse)	1:100	BP106, Developmental Studies Hybridoma Bank (DSHB)
Anti-Arm (mouse)	1:100, 1:500*	N27A1, DSHB
Anti-DE-cad (rat)	1:100	DCAD2, DSHB
Anti-Dlg (mouse)	1:500, 1:1000*	4F3, DSHB
Anti-Cno (rabbit)	1:1000	J. Sawyer and N. Harris (University of North Carolina at Chapel Hill)
Anti-Baz (rabbit)	1:2000, 1:1000*	(Choi et al., 2013)
Anti-Scrib (guinea-pig)	1:500, 1:1000*	(Zeitler et al., 2004)
Anti-Par-1 (guinea-pig)	1:800	(McDonald et al., 2008)
Anti-Rab5 (guinea-pig)	1:1000	(Tanaka and Nakamura, 2008)
Anti-Zip (rabbit)	1:500	(Chougule et al., 2016)
Anti-α-Tubulin (mouse)	1:4000, 1:5000*	T6199, Sigma Life Science
Phalloidin Alexa 488	1:500	A12379, Thermo Fisher Scientific
Anti-Afadin (rabbit)	1:500, 1:1000*	A0224, MilliporeSigma
Anti-Afadin (mouse)	1:100	610732, BD Biosciences
Anti-Scribble (mouse)	1:100, 1:1000*	7C6.D10, MAB1820, MilliporeSigma
Anti-Scribble (rabbit)	1:500	PA5-66680, Thermo Fisher Scientific
Anti-c-myc (mouse)	1:100, 1:1000*	SC-40, SCBT
Secondary antibodies		
Alexa 488, 568, and 647	1:500	Life Technologies
IRDye 680RD and RDye 800CW	1:10,000	Licor Biosciences

Table S2. Summary of data replicates

Figure	Measurement	Genotype	Stage	*n* (embryos)	Quantification panel
Fig. 1	Dlg enrichment at the level of the AJ	WT	5 *late*	5	1I
	Scrib enrichment at the level of the AJ	WT	5 *late*	7	1I
	Apical-basal Scrib intensity with respect to AJ intensity	WT	5 *late* 6 *mid* 7 10	4 3 4 1	1H 1J 1K 1B
Fig. 2	Dlg apical intensity, Dlg apical focusing (scored in text)	WT	*5 late/6 early*	22	2G,N
		Rap1 RNAi	*5 late/6 early*	8	2G
		baz RNAi	*5 late/6 early*	9	2G
		arm RNAi	*5 late/6 early*	11	2N
Fig. 3	Basolateral spread of Arm	WT	5 *mid-late* *6 late/7*	13 8	3G,H 3L
		scrib RNAi	5 *mid-late* 6 *late/7*	11 6	3G,H 3L
		dlg1 RNAi	5 *mid-late* 6 *late/7*	16 7	Not quantified
Fig. 4	Basolateral spread of Cno	WT	5 *mid-late* 6 *late/7*	18 11	4I,J 4P
		scrib RNAi	5 *mid-late* 6 *late/7*	17 9	4I,J 4P
		dlg1 RNAi	5 *mid-late* 6 *late/7*	9 5	Not quantified
Fig. 5	Baz cortical intensity	WT	5 *late* 6	5 3	5C Not quantified
		scrib RNAi	5 *late* 6	3 5	5C Not quantified
	Baz apical enrichment	WT	5 *late* 6 *late/7*	4 5	5D,G Not quantified
		scrib RNAi	5 *late* 6 *late/7*	6 7	5E,G Not quantified
		Rap1 RNAi	5 *late*	6	5F,G
Fig. 7	Cortical localization of Par-1	WT	5 *late/6 early*	7	7E,F
		scrib RNAi	5 *late/6 early*	5	Suppl. Fig. 6I,J
		dlg1 RNAi	5 *late/6 early*	5	7E,F
	Basolateral spread of Arm, Cno	WT	5 *mid-late*	4	7Q
		par-1 RNAi	5 *mid-late*	7	7Q
Fig. 8	Expansion of junctional zone	WT	5 late/6 *early* 6 *mid* - 7	5 9	8Q,R Not quantified
		scrib^{4}	5 late/6 *early* 6 *mid* - 7	4 10	8Q,R Not quantified
Fig. 9	Detection of biotinylated Scrib by western blot	AF-6-BirA/ BirA-AF-6	2 independent experiments		9F

Entries in this table represent data that was quantified unless indicated. For more qualitative observations multiple embryos of each genotype (generally more than 20) were observed and if there was significant variability this was reported in the text.